Computational-Experimental Study of Plasma Processing of Carbides at High Temperatures

Arturo Bronson and Vinod Kumar
Department of Mechanical Engineering
University of Texas at El Paso

Program Manager: Richard J. Dunst

National Energy Technology Laboratory

DOE Award – FE0008400

High Temperature Research Group

- **Graduate Students**
  - **Alejandro Garcia (Computational - Masters)**
  - **Arturo Medina (Computational - Masters)**
  - **Sanjay Shantha-Kumar (Experiment - Ph.D.)***
- **Senior Students**
  - **Alberto Delgado (Experimental – Mechanical / Metallurgical Engineering)**

*** Aids students in high temperature research.**

Motivation/Impact of Research

- Use electromagnetics to control plasma surface reactions.
- Use plasma processing to create temperature extremes.
- Use temperature spikes to form metastable phases.
- Use electromagnetics to change diffusional flux.

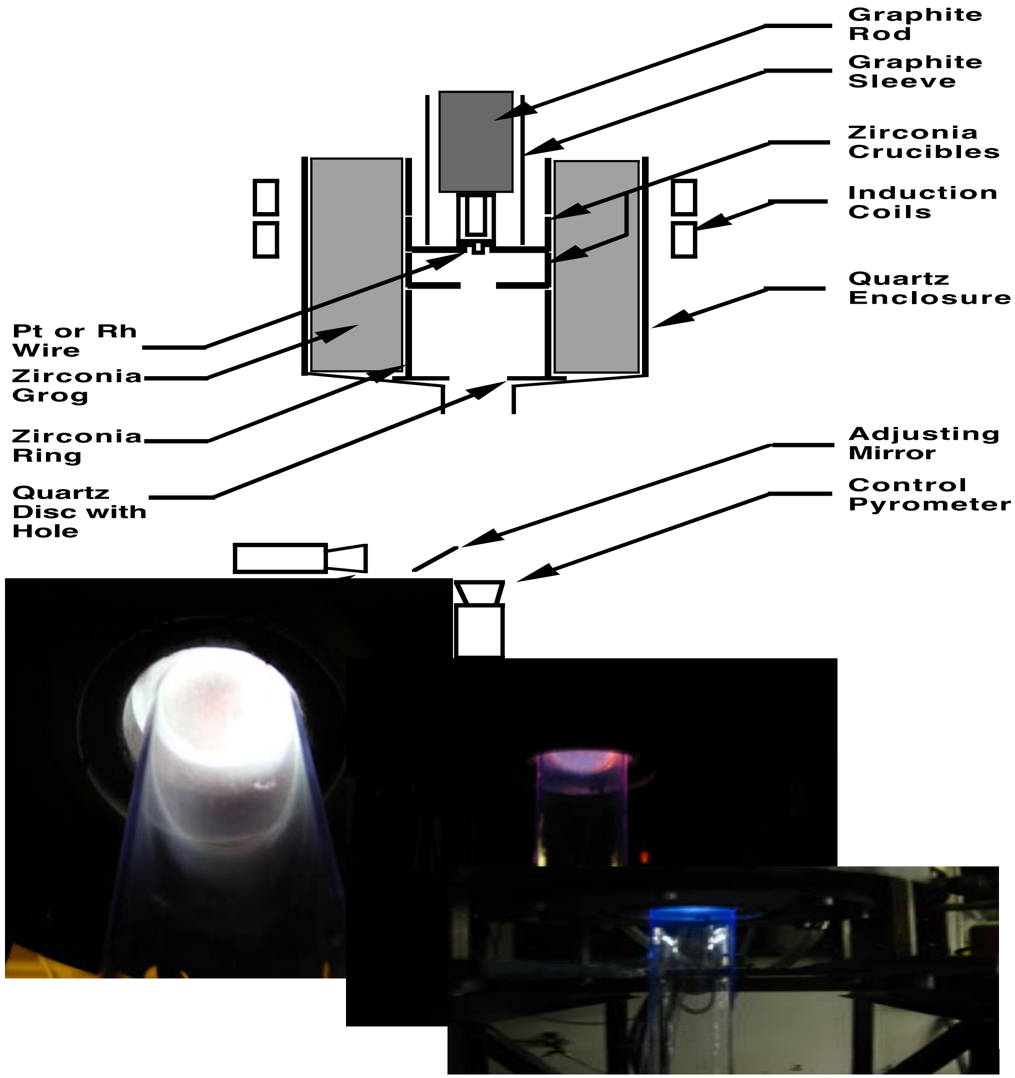

Outline of Presentation

- Introduction – Processing
  - Scale of SiO_2, Al_2O_3 and TiO_x
  - Vaporization/Surface Kinetics
  - Packed Bed Reactivity
  - Plasma Surface Reactions
- Computational Effort – thermodynamics and heterogeneous kinetics using plasma gas
- Strategic Experimentation – SiC, $ZrC-TiO_2-Y_2O_3$, $Ti_2AlC-TiC-Y_2O_3$
- Progress and Analysis

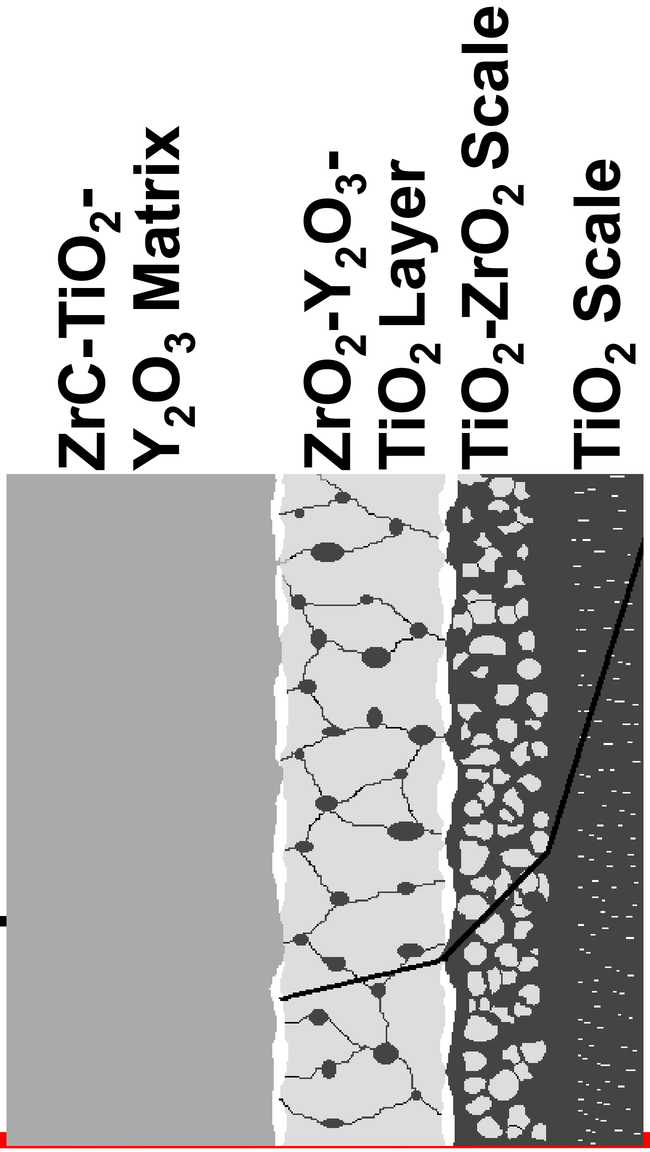

Kellogg Diagram for Ti-O System (2500 K)

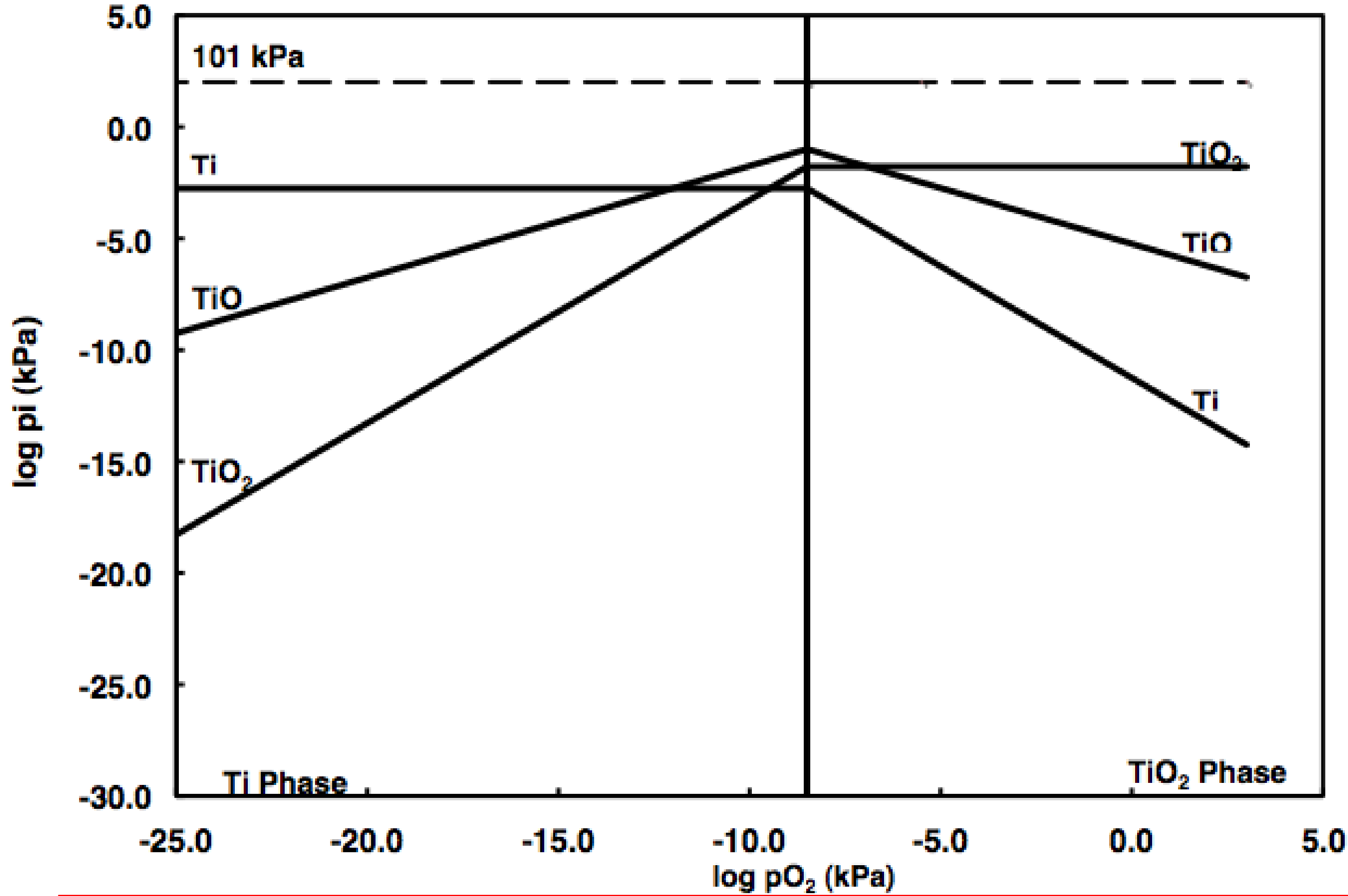

Vaporizing Flux of SiO_2 and TiO_2

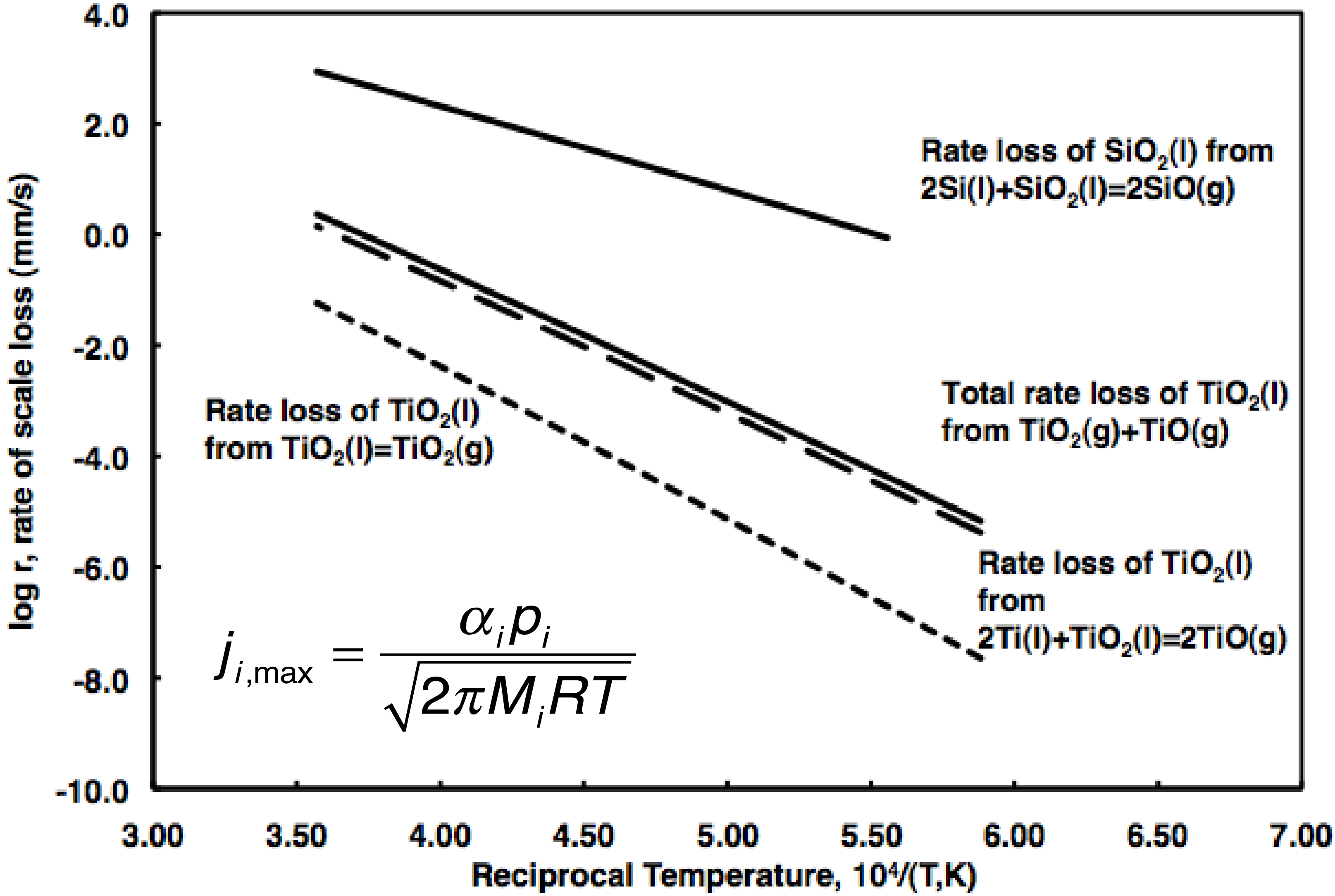

Project Objectives

- Investigate the effects of plasma surface reactions within pores of carbide packed bed;
- Investigate the effect of the potential gradients of the electromagnetic field on mass transfer;
- Investigate the effect of temperature spikes on pore surfaces.

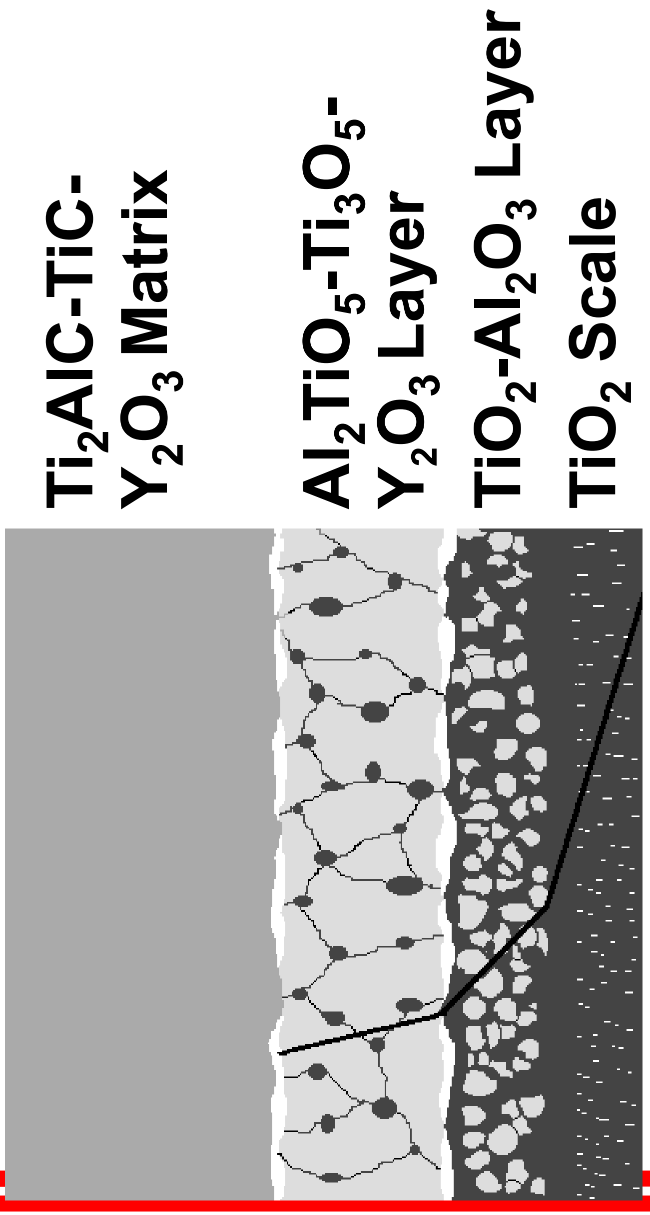

Oxygen Permeability

- For temperatures between 1700 to 1500° C Al_2O_3 and Y_2O_3 have oxygen permeability ≤ 10^{-9} $gO_2/(cm\text{-}s)$ and $3 \cdot 10^{-9}$ $gO_2/(cm\text{-}s)$, respectively.
- Oxygen permeability of ZrO_2-Y_2O_3 and HfO_2-Y_2O_3 increases by approximately an order of magnitude [i.e., ≥ $(10)^{-8}$ $gO_2/(cm\text{-}s)$].

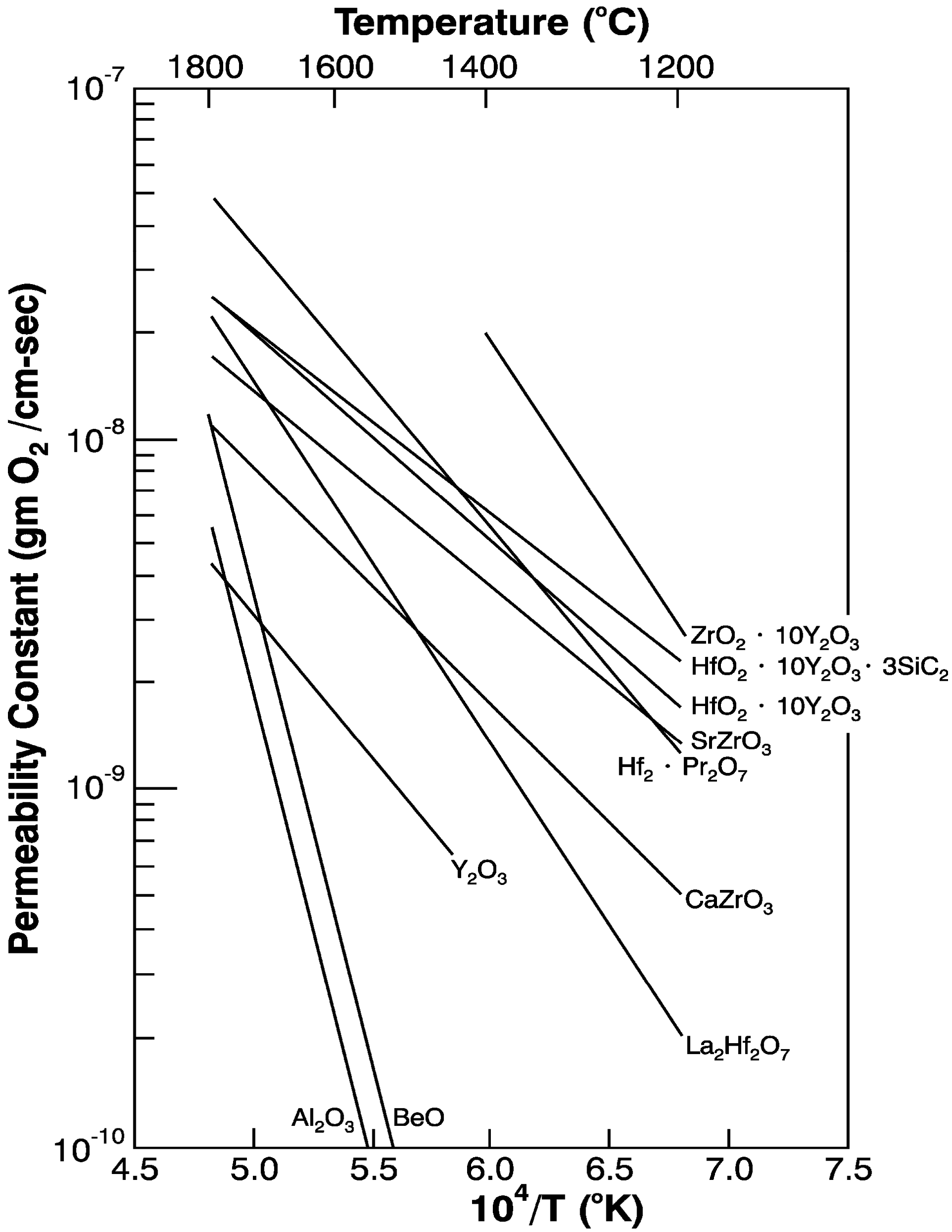

(Opeka, Talmy & Zaykoski-2004)

Stabilities-Oxides and Carbides

- For carbides, HfC, Ta_2C and ZrC are most stable.
- For oxides, Y_2O_3 and HfO_2 are most stable.
- Used Outotec HSC v. 7

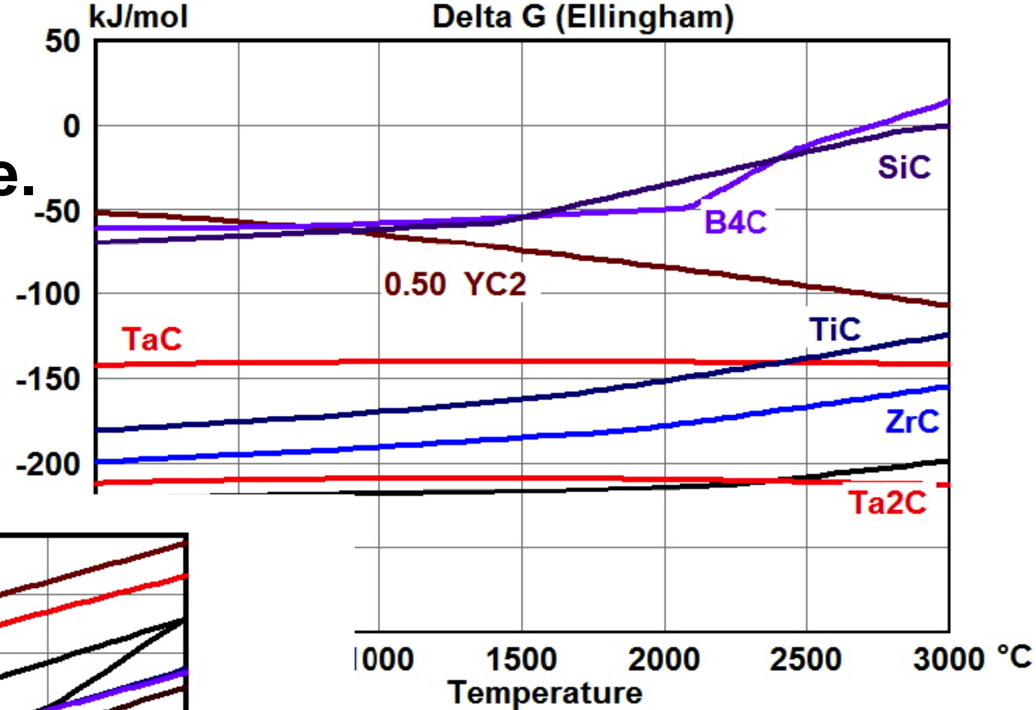

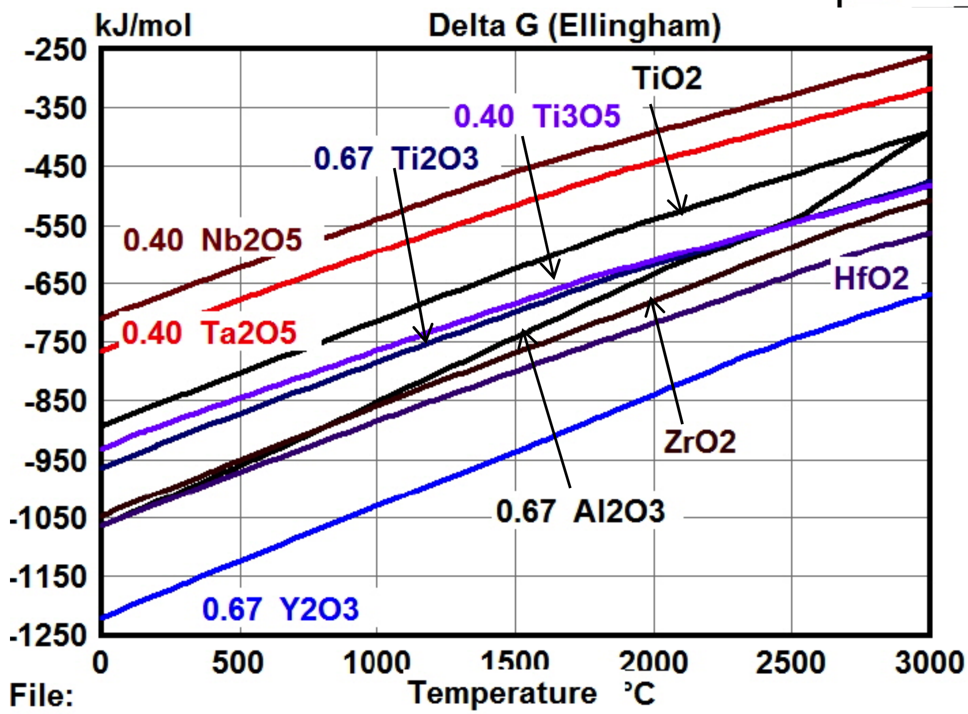

Ti-C-O Stability Diagrams at 1273 & 1973K for Expanded View of Magneli phases & p_{O2}

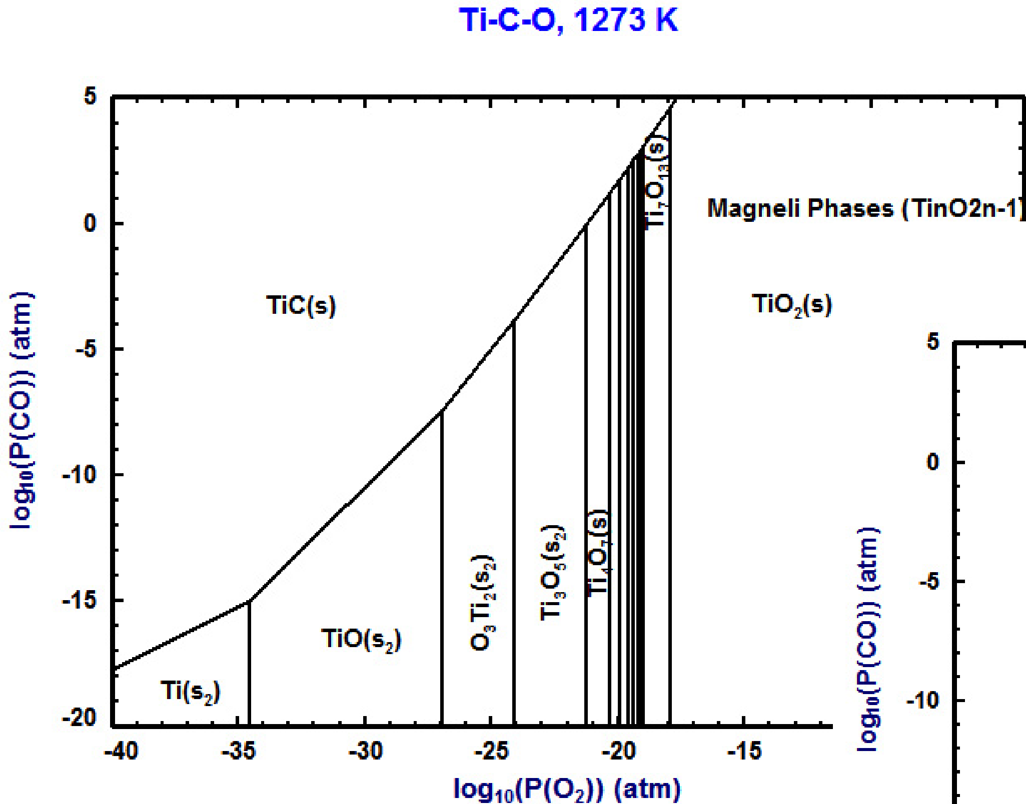

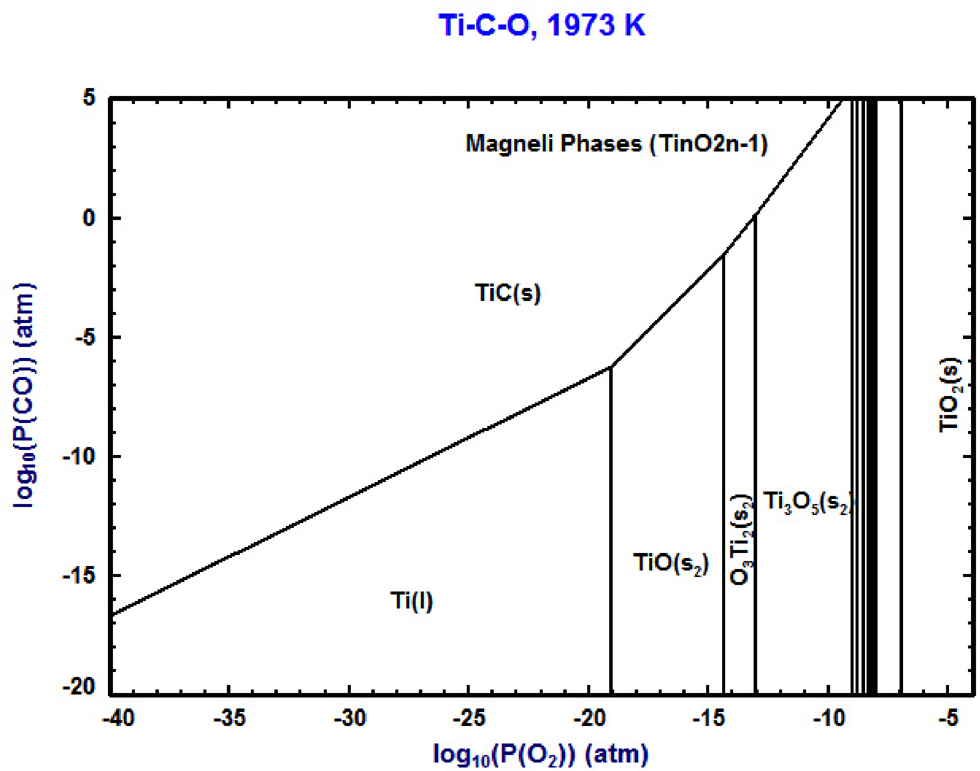

Possible Scale of Oxidized Ti_2AlC-TiC

- **Ti oxides depend on pO_2 level within scale.**
- **Muan/Osborn showed limited solubility of Al_2O_3 - Al_2O_3•TiO_2 and Al_2O_3•TiO_2 - TiO_2 pseudobinaries.**
- **Al_2O_3•TiO_2 melts congruently at 1860° C as per Muan/Osborn.**

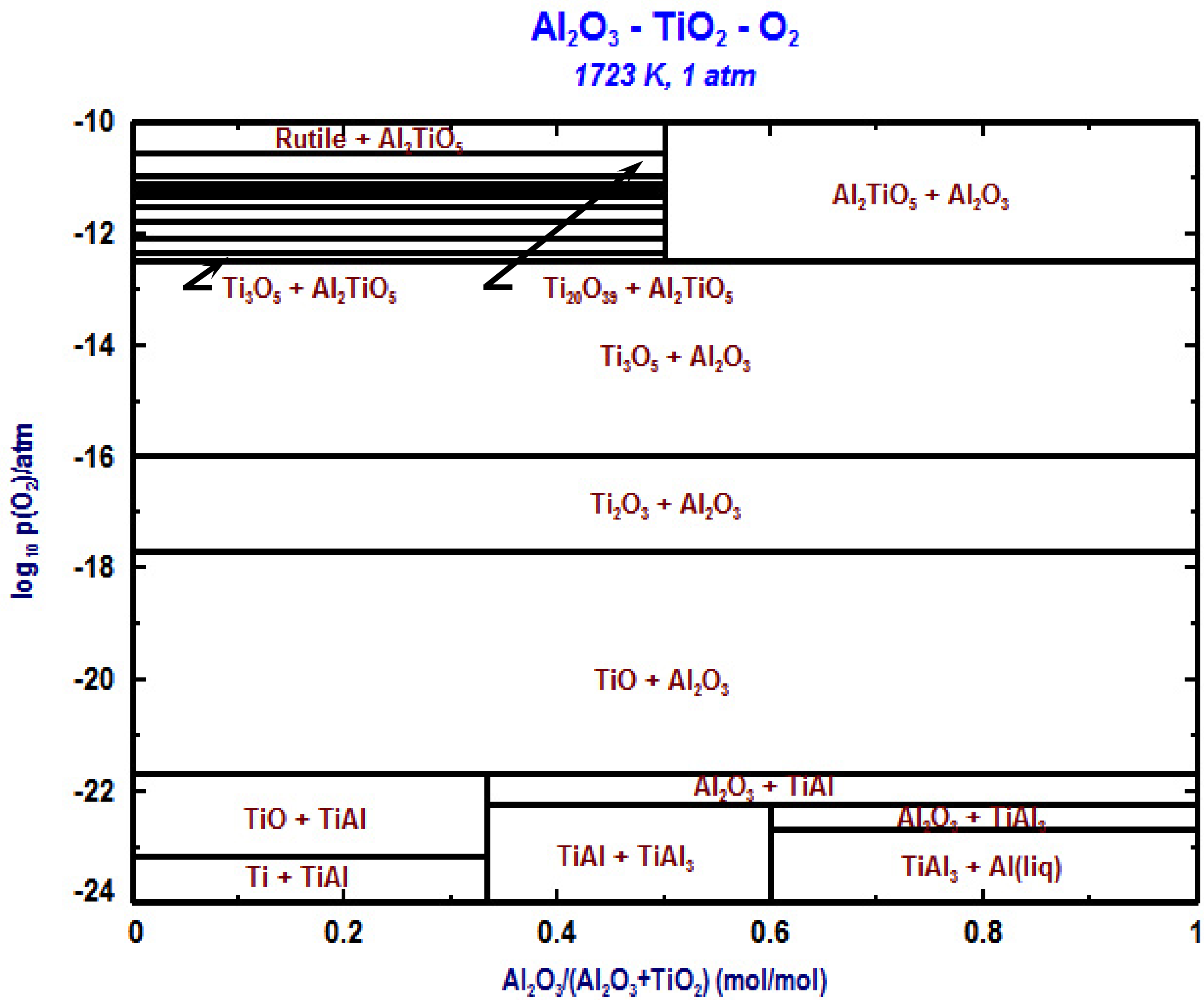

COMSOL Simulation of B_4C Spheres Basis for Packed Bed with Temperature Profile

- Carbide spheres configured in an X-pattern rotating along centerline.
- The spheres have an open structure.

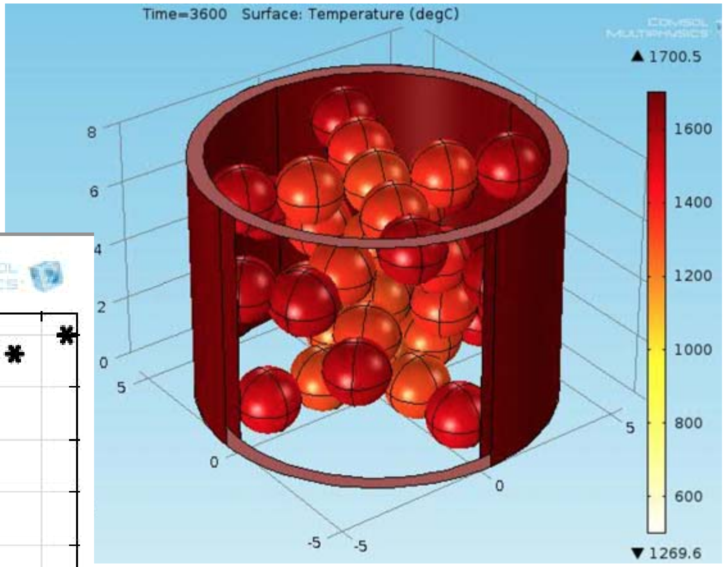

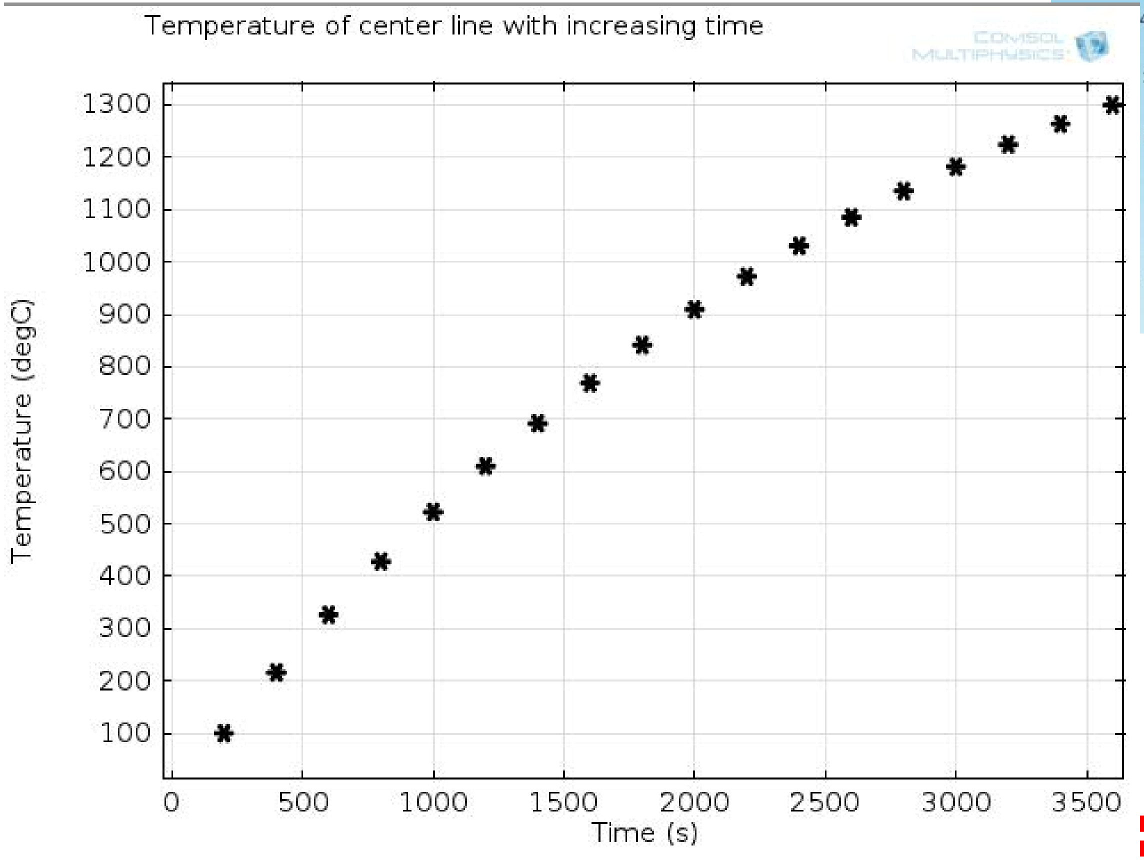

COMSOL Simulation of B_4C spheres in a packed bed

- Cylindrical graphite wall temperature is heated mimicking internal furnace wall.
- Carbide spheres touch each other with a 6-fold lateral configuration though each layer contacts uniformly.
- Spheres contacting the wall have highest temperature.
- Conductive heat transfer was used, but radiation will be added with expanded sphere number.

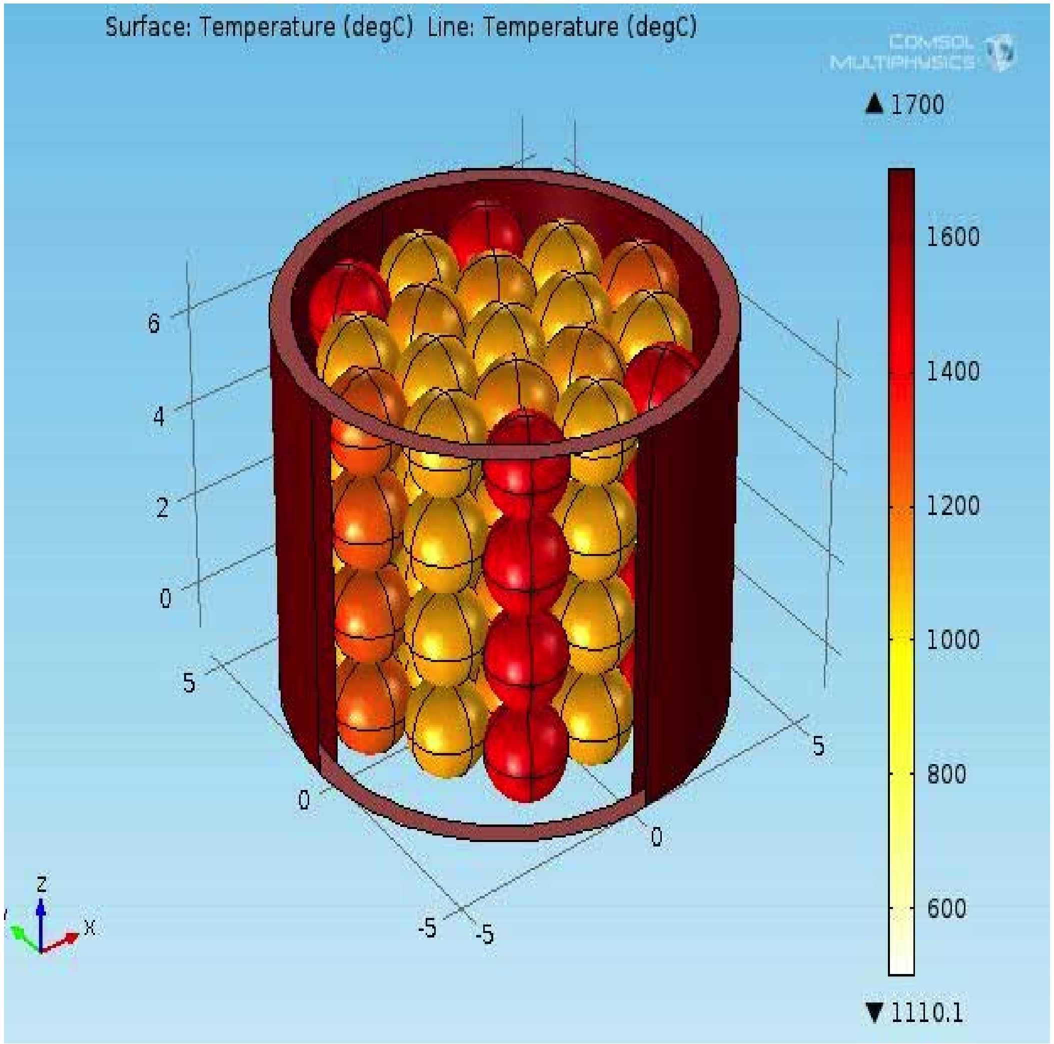

Extending Previous Kinetic Equations

- Grabke's equations [1965 and 1970] for oxygen transfer on metals (e.g., Fe)

$$\frac{dn_O}{dt} = ka_O^{-m} p_{CO2} - ka_O^{1-m} p_{CO}$$

- Wang et al. [2003] determined oxidizing sequence for Ti44Al11Nb alloy with X-ray photoelectron spectroscopy.

$$O_2 + 2V = 2O_{ad}$$

$$Al + O_{ad} \rightarrow AlO$$

$$AlO + O_{ad} \rightarrow AlO_2$$

$$AlO_2 + O_{ad} \rightarrow AlO_3$$

- Kurunczi, Guha and Donnelly [2006] on adsorption of oxygen (O_{ads}) on surface sites (V) from O2 plasma

$$Og + V \rightarrow O_{ads}$$

$$2O_{ads} \rightarrow O_{2(g)} + 2V$$

Oxidized Species Measured on Ti-44Al-11Nb (at%) with X-ray Photoelectron Spectroscopy

- **Oxygen exposure of L = t•p_{O2} (10^{-6} Torr•s)**
- **Slope of 2/3 acquired from kinetic rates of oxygen adsorption per AlO_3 formation (r_{ad}/r_{AlO3})**

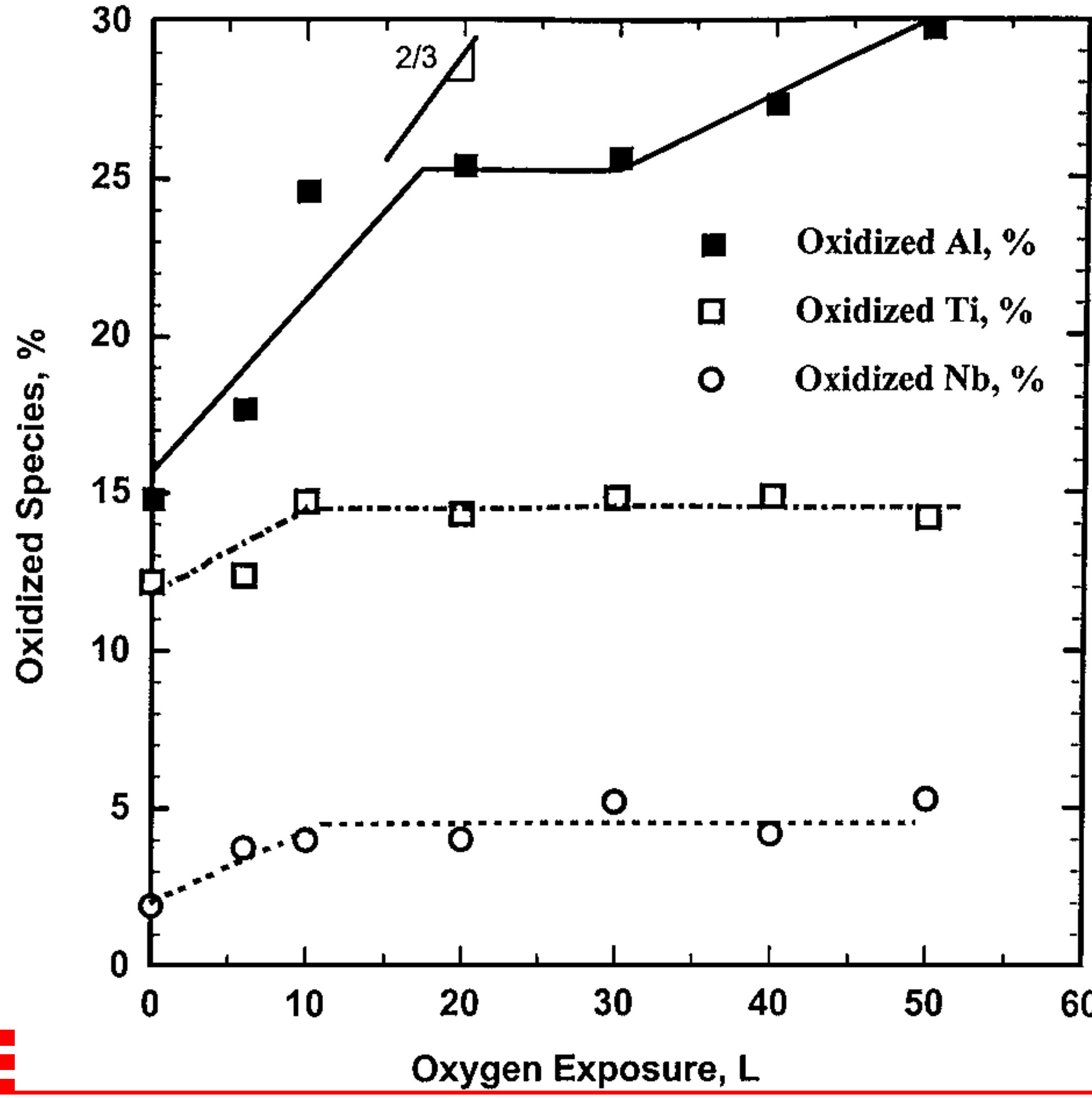

Future Efforts for Plasma Surface Reactions

- **Incorporate electron energy** **(e.g., electron energy density (*n_ε*), gradient of electron flux vector (Γ_ε) and potential field (E)).**

$$\frac{\partial}{\partial t}(n_\mathcal{E}) + \nabla \cdot \Gamma_\mathcal{E} + \mathbf{E} \cdot \Gamma_\mathcal{E} = \ R_\mathcal{E} - (\mathbf{u} \cdot \nabla) n_\mathcal{E}$$

- **Incorporate kinetics of Ar-O_2 plasma-surface reactions with SiC and Ti_2AlC.**
- **Study the effect of temperature extremes (T and dT/dx) on metastable phases and/or segregation.**

Summary

- Analyzed thermodynamic stability of oxygen potentials for TiO_x and TiO_x-Al_2O_3 for possible scale formation from Ti_2AlC-TiC components.
- Using primarily COMSOL, a commercial software package, incorporating the modules of heat transfer, kinetics, plasma as well as its material database to model surface plasma reactions.
- Incorporating the oxidation of Ti-Al-M as a basis for the plasma-surface reactions.
- Determining the effect of charged surface sites attracting ultimately the oxygen for surface reactions.

Questions and Comments

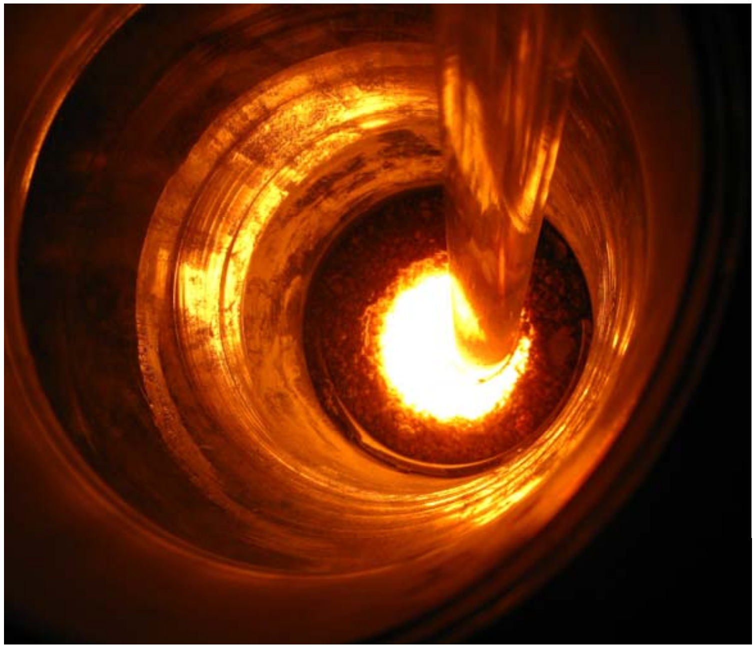

Slides to Respond to Possible Queries Follow

Wagner's Rate Equation for Scales

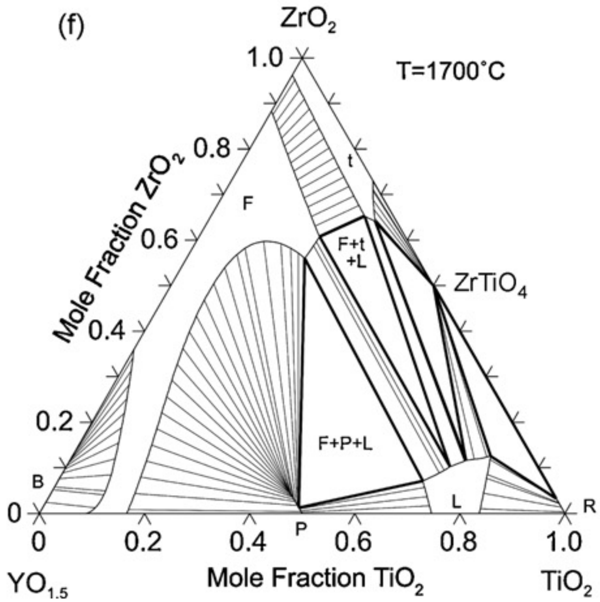

Calculated Diagram from Schaedler, Fabrichnaya and Levi -- 2008

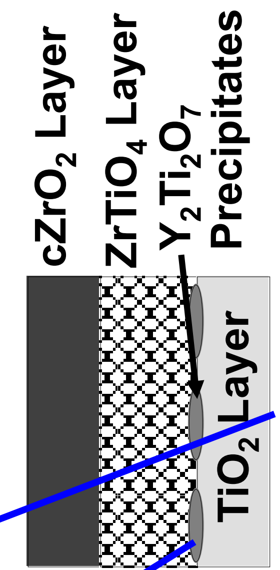

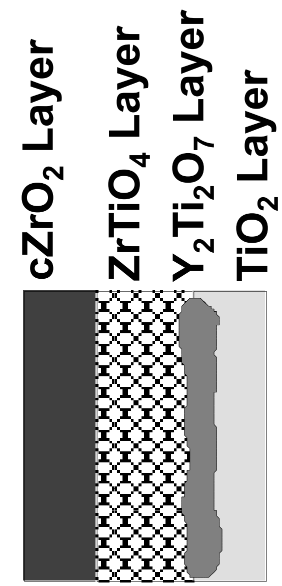

$$\frac{1}{A}\frac{d\tilde{n}}{dt} = \frac{1}{\xi}\left[\frac{\tilde{c}}{2}\int_{p_{O_2}^{(i)}}^{p_{O_2}^{(o)}}\left(\left(\frac{z_M}{z_O}\right)D_M + D_O\right)d\ln p_{O_2}\right] = \frac{\tilde{k}}{\xi}$$

Parabolic Growth Rate of Scale

- $D_{eff} = 10^{-11} m^2/s$ for t-ZrO_2-Y_2O_3 phase as controlling layer

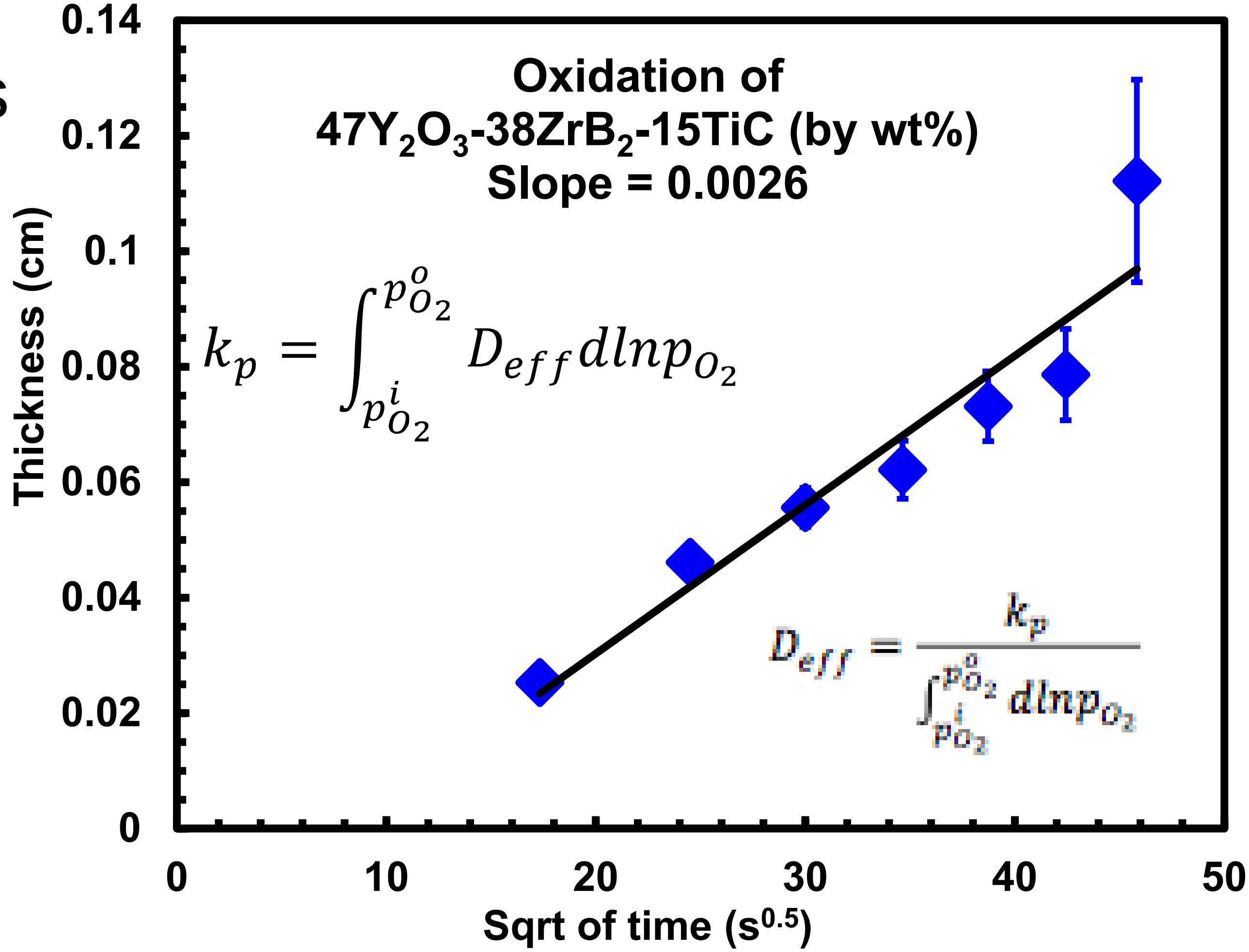

$$k_p = \int_{p_{O_2}^i}^{p_{O_2}^o} D_{eff}\, d\ln p_{O_2}$$

$$D_{eff} = \frac{k_p}{\int_{p_{O_2}^i}^{p_{O_2}^o} d\ln p_{O_2}}$$

Electron-Energy Transport

- Should consider electron, ions and neutral species balance coupled with electron energy and momentum balances.

$$\frac{\partial}{\partial t}(n_\varepsilon) + \nabla \cdot \Gamma_\varepsilon + \mathbf{E} \cdot \Gamma_\varepsilon = R_\varepsilon - (\mathbf{u} \cdot \nabla) n_\varepsilon$$

$$\frac{\partial}{\partial t}(n_e) + \nabla \cdot [-n_e(\mu_e \cdot \mathbf{E}) - \mathbf{D}_e \cdot \nabla n_e)] = R_e$$

Kellogg Diagram for Si-O System (2500 K)

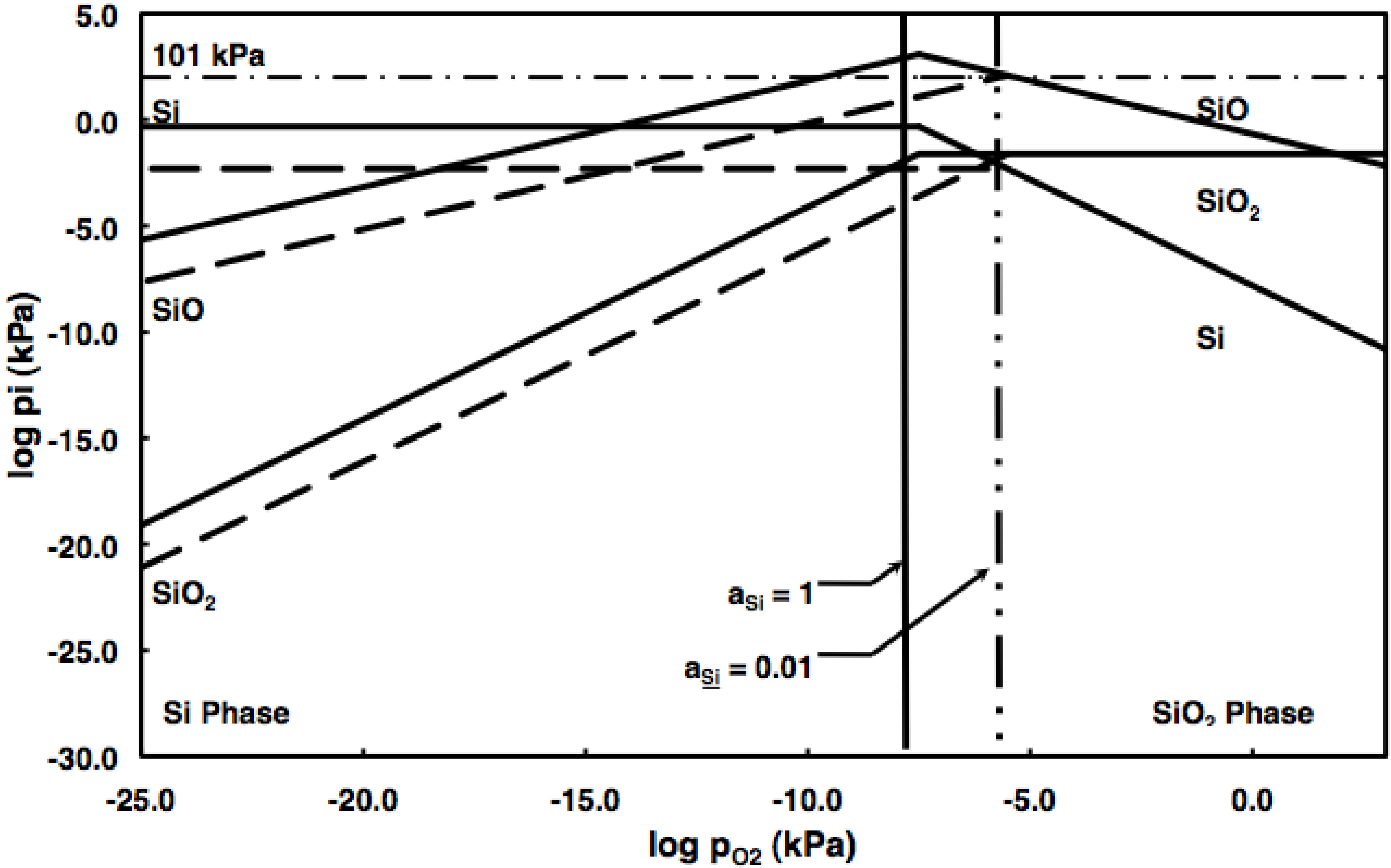

SEM image after spark-plasma sintering

- ZrB_2 oxidizes to ZrO_2 dissolving some Y_2O_3
- Stringers of Y_2O_3 appear in grain boundary
- Graphite seems to minimize TiC oxidation.

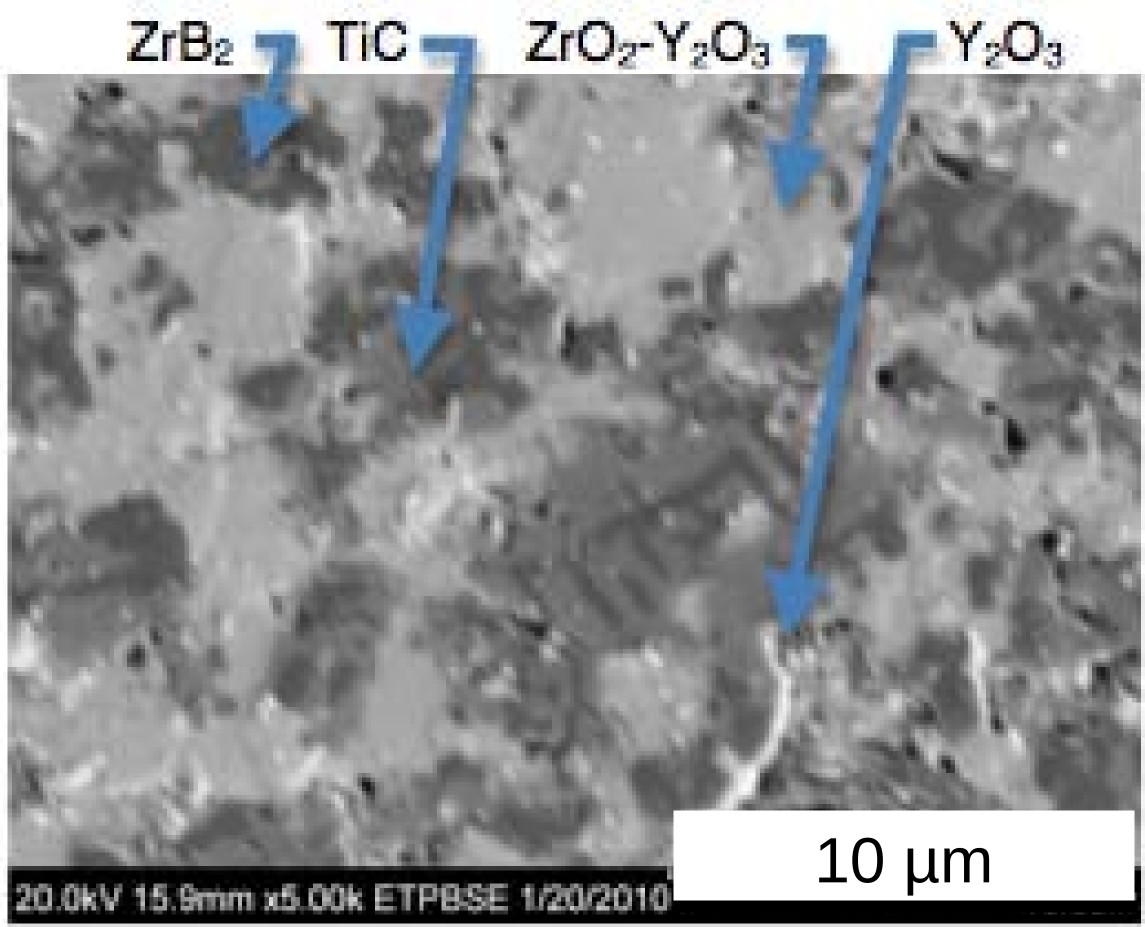

Oxidation in Silicide Furnace with air and C/CO/N_2 atmospheres at 1700° C

- Spark plasma-sintered samples
- ZrO_2-8 wt% Y_2O_3 crucible covers were used to hold samples.
- Hf foil were also used to hold samples.

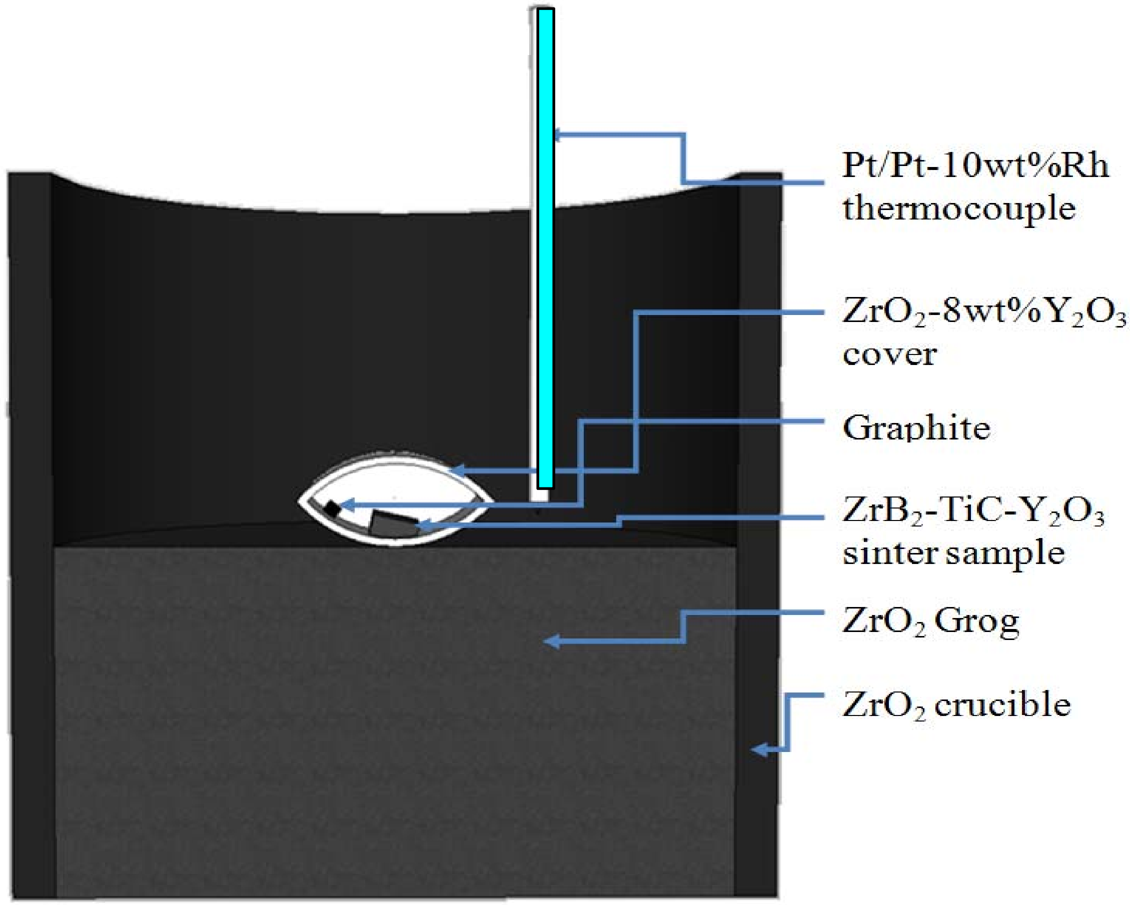

Oxygen Levels for TiO_x with Calculated $Ti-ZrB_2-O_2$ Phase Diagram

- Ti oxides start to form near $p_{O2} > 10^{-22}$ atm with TiO.
- Ti_2O_3/Ti_3O_5 has $p_{O2} = 10^{-15.5}$ atm
- ZrB_2 oxidizes to t-ZrO_2 with Ti oxides.
- Liquid oxides form with increasing p_{O2}

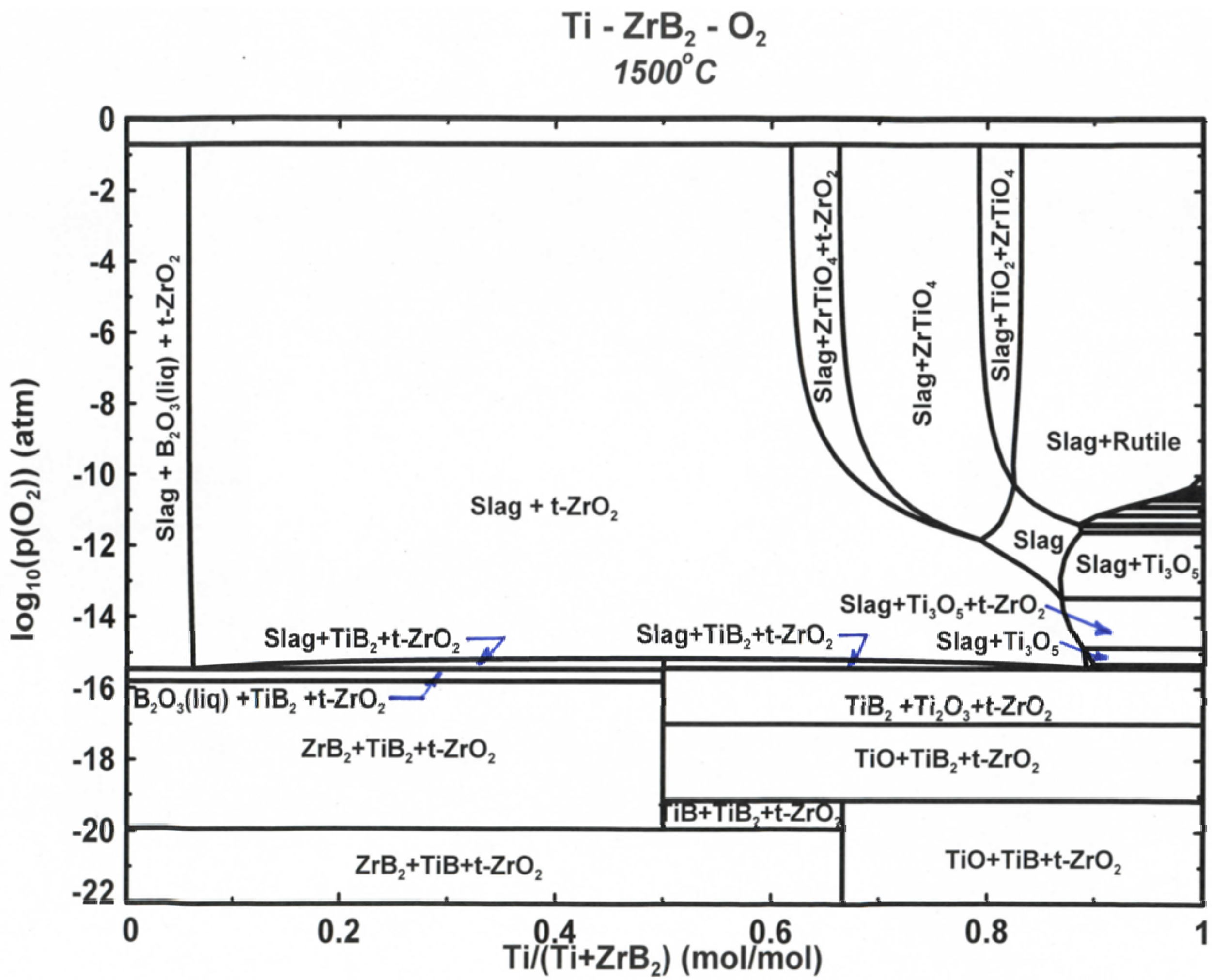

Optical Microstructures to Measure Scale

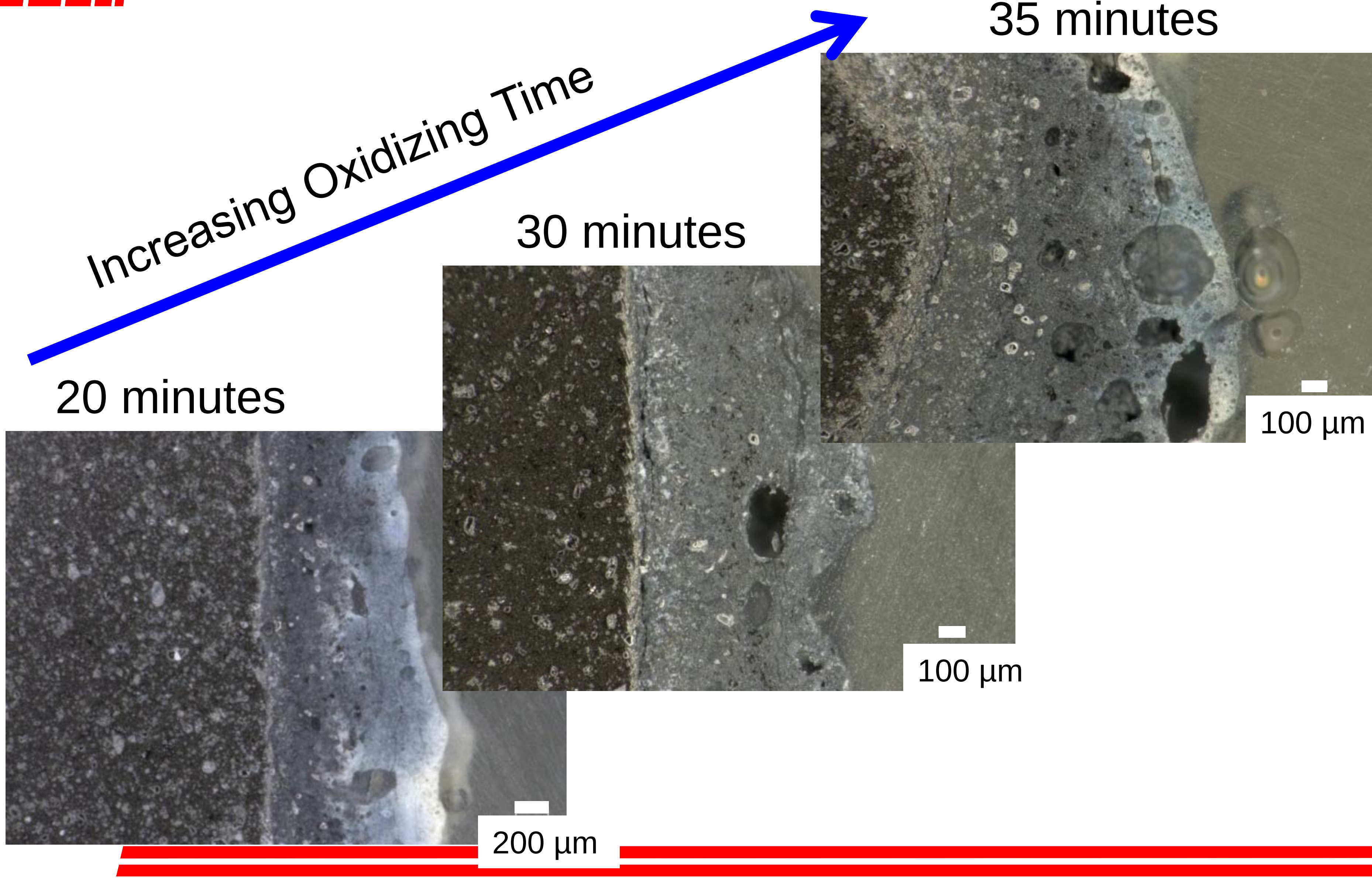

Oxidized $30ZrB_2$-13TiC-$37Y_2O_3$-20Ta sample for 3 minutes at 1700° C

- Oxidized area becomes ZrO_2-TiO_2-Y_2O_3
- Ta forms Ta_2O_5 upon oxidation with vaporization

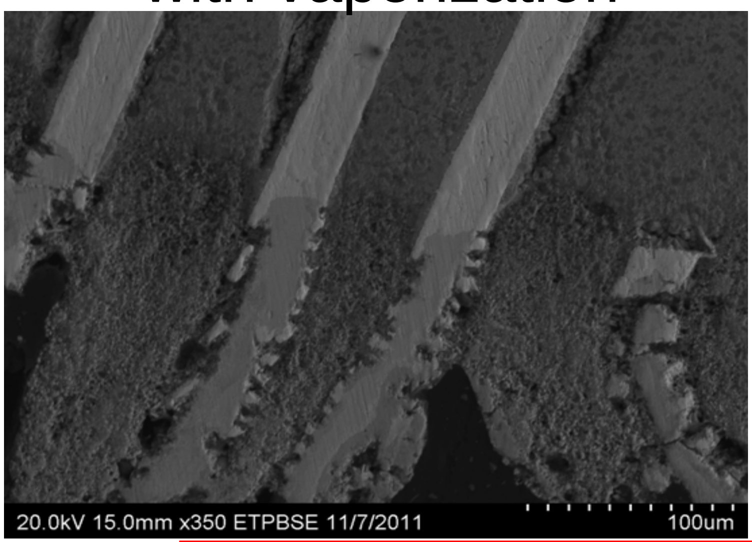

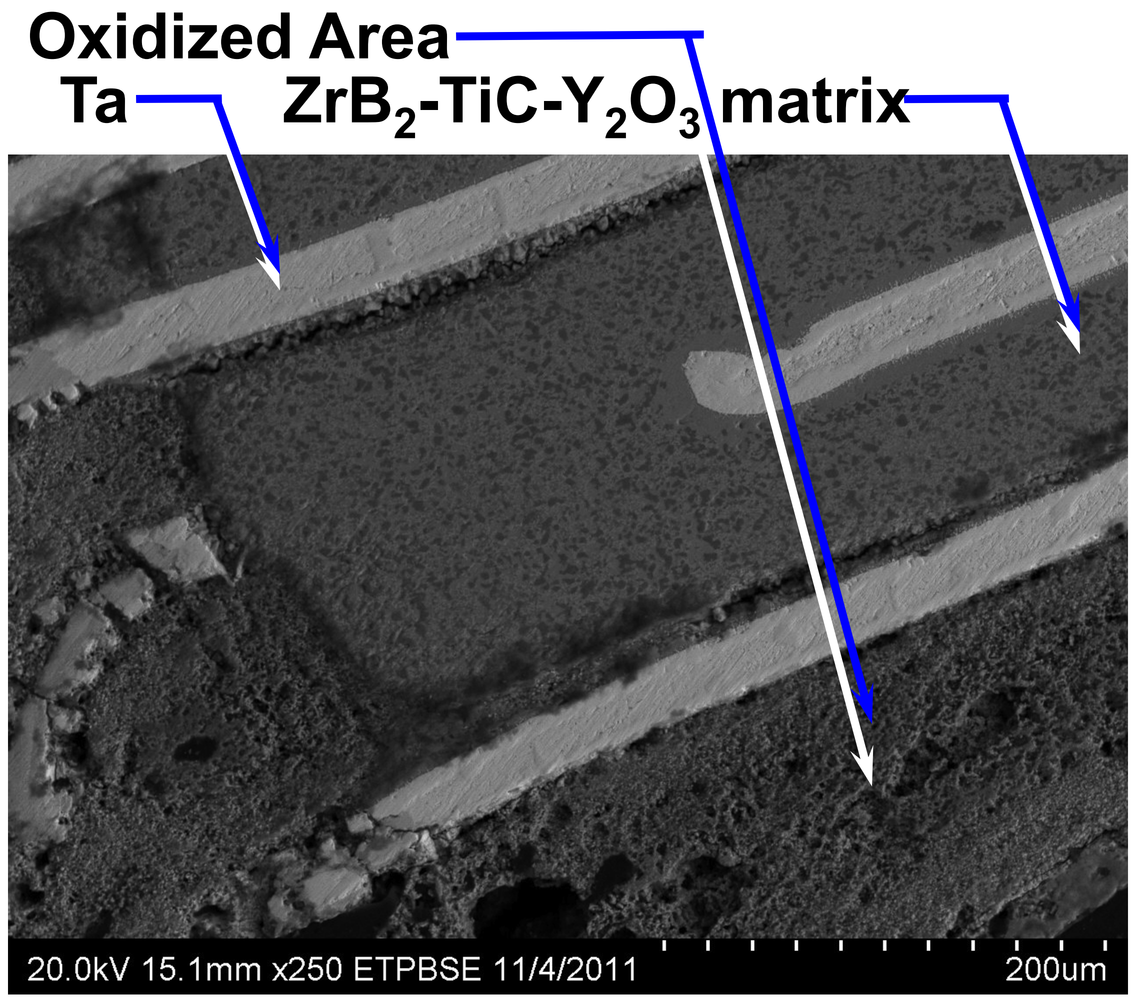

Ta_2O_5-TiO_2 phase diagram

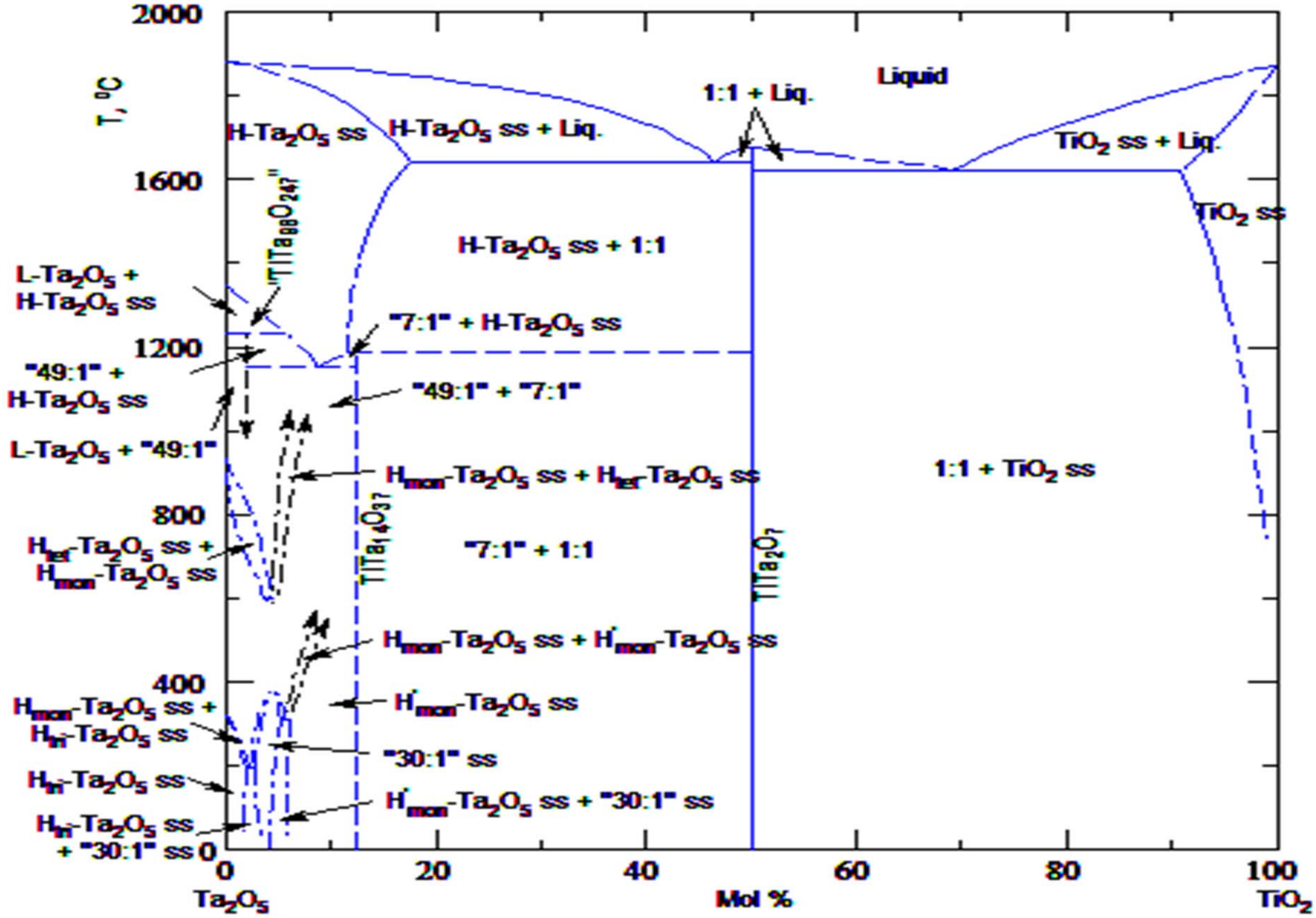

Remodeling Departmental Materials and Structures Laboratory (Dynamic)

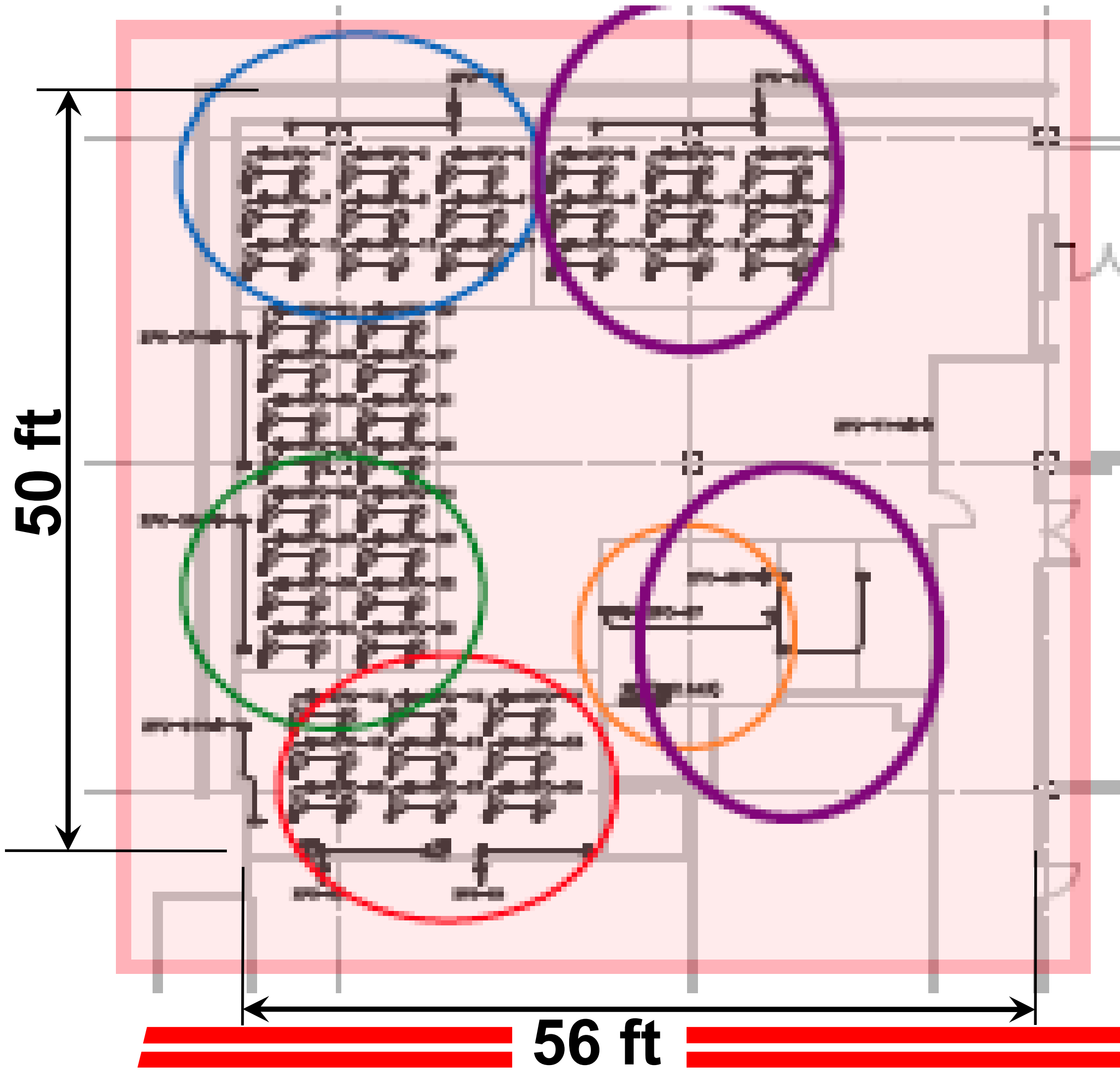

- Other than standard 120VAC, will need:3-phase,
- 480 VAC in Bay 2 (encircled - blue)120A,
- 3-Phase, 240VAC in Bay 4 (encircled - green) 40A,
- Single Phase, 210VAC in Bay 5 (encircled – red)50A,
- 3-Phase, 240VAC in Bay 5 (encircled - red)50A,
- 3-Phase, 240VAC in Bay 6 (orange) Purple Area .

Seek DURIP Request for Ultra-high Temperature Furnace

- **Dielectric induction furnace (3-7 MHz) reaching 2600 or 3500° C**
- **Four Infrared pyrometers**
- **Support AFOSR/ONR efforts**

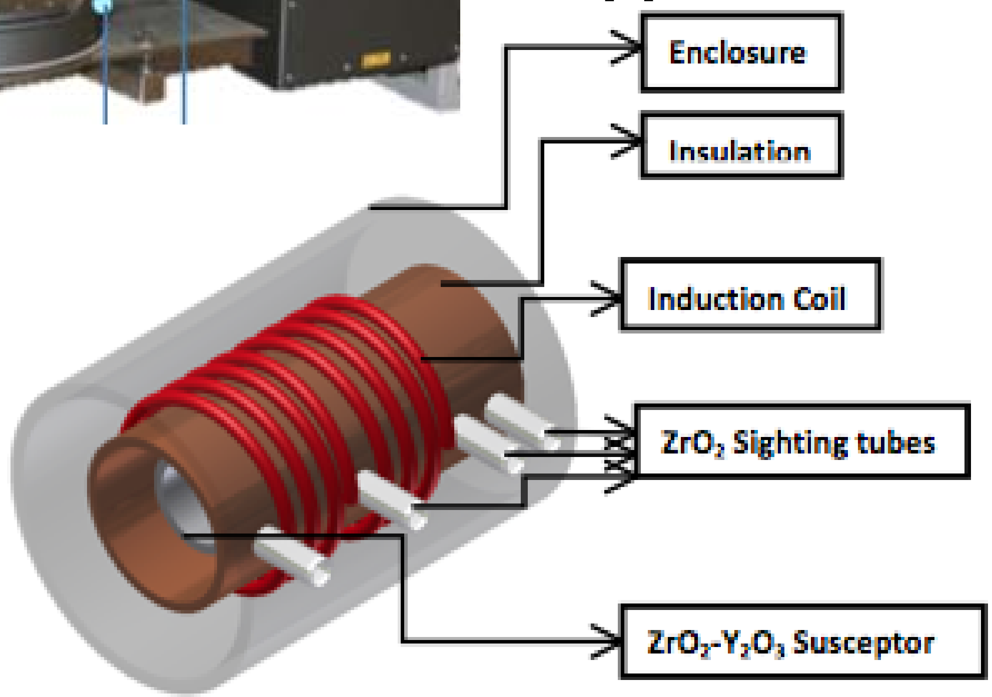

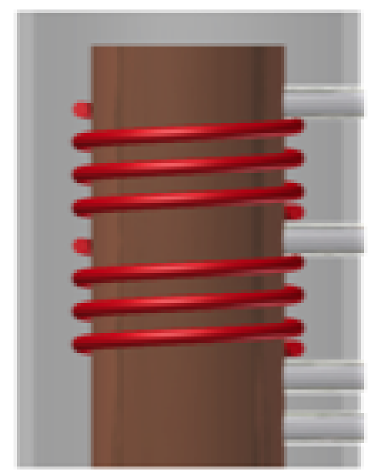

Phases identified for oxidized sample in $C/CO/N_2$

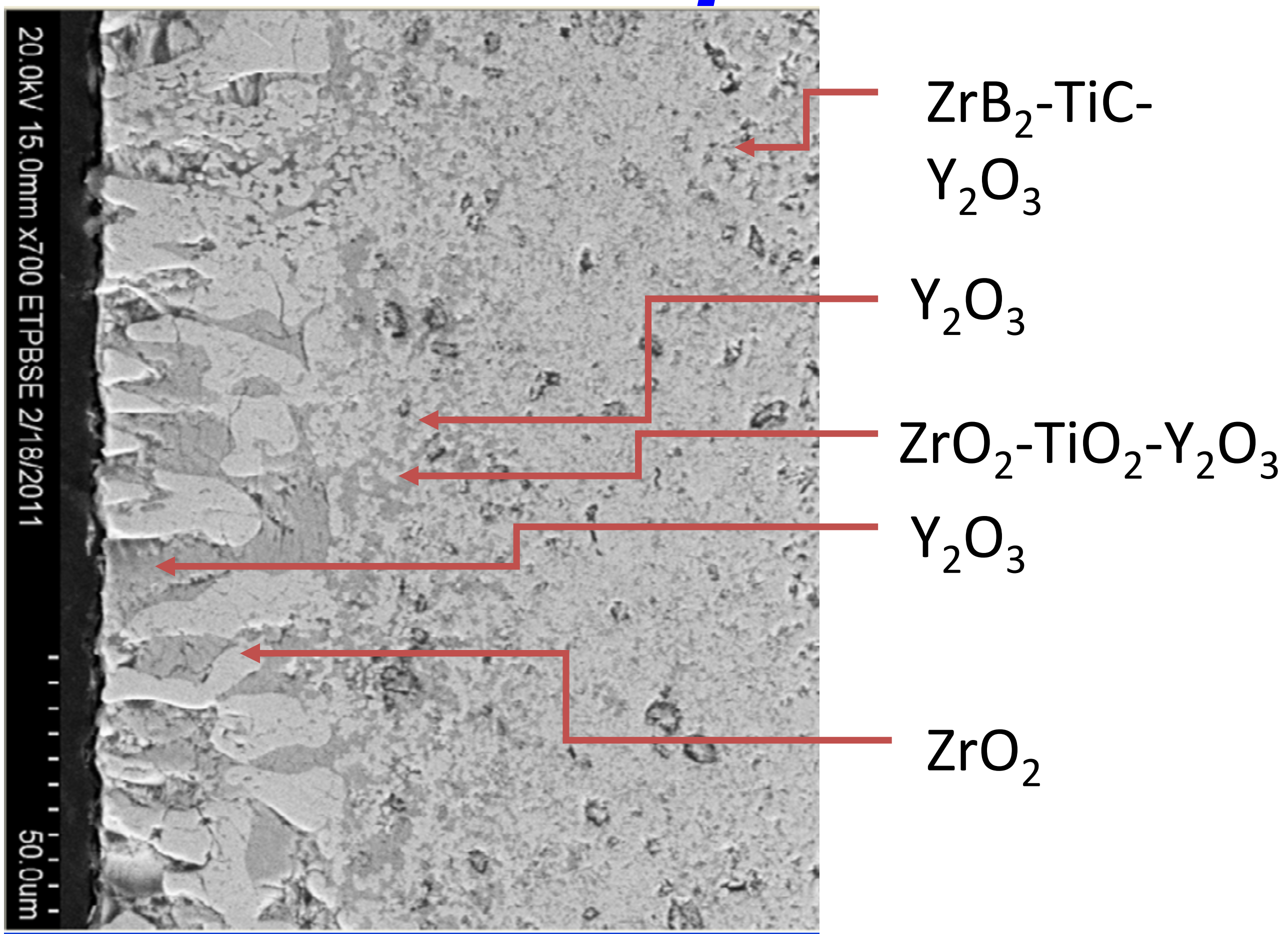

Calculated Zr-Ta-O_2 and Ti-Ta-O_2 phase diagrams

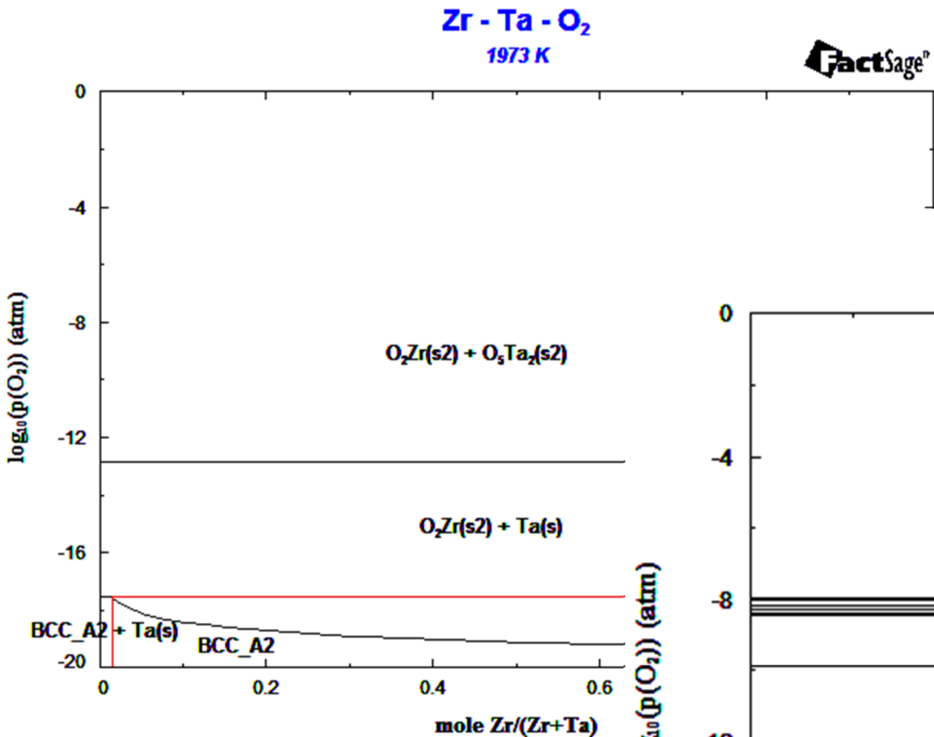

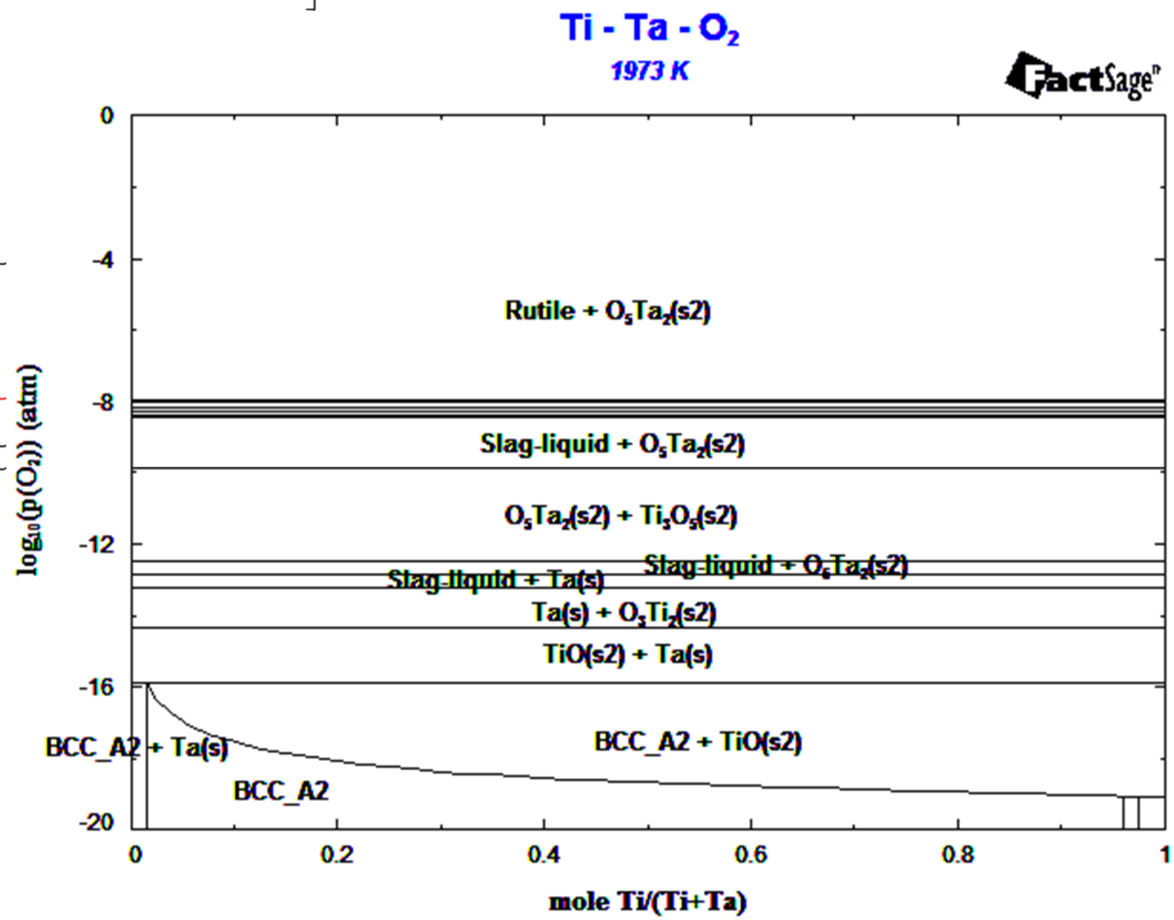

- p_{O2} level for Ta/Ta_2O_5
- $TiOx\text{-}Ta_2O_5$ liquids

Zr as primary component in B_4C reaction on Zr-B-C phase diagram

- Zr liquid changes with alloy composition
- Zr reacts with B_4C forming ZrC and ZrB_2 as a result of the mass balance.

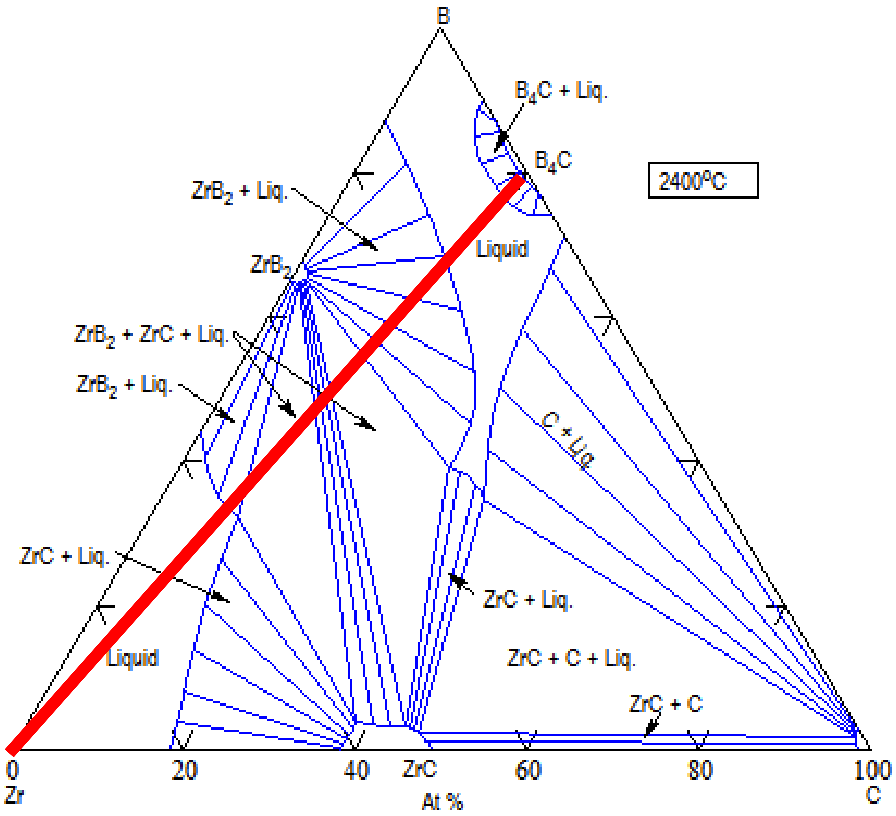

Ti-Zr-O_2 Phase Diagram at 1973 K

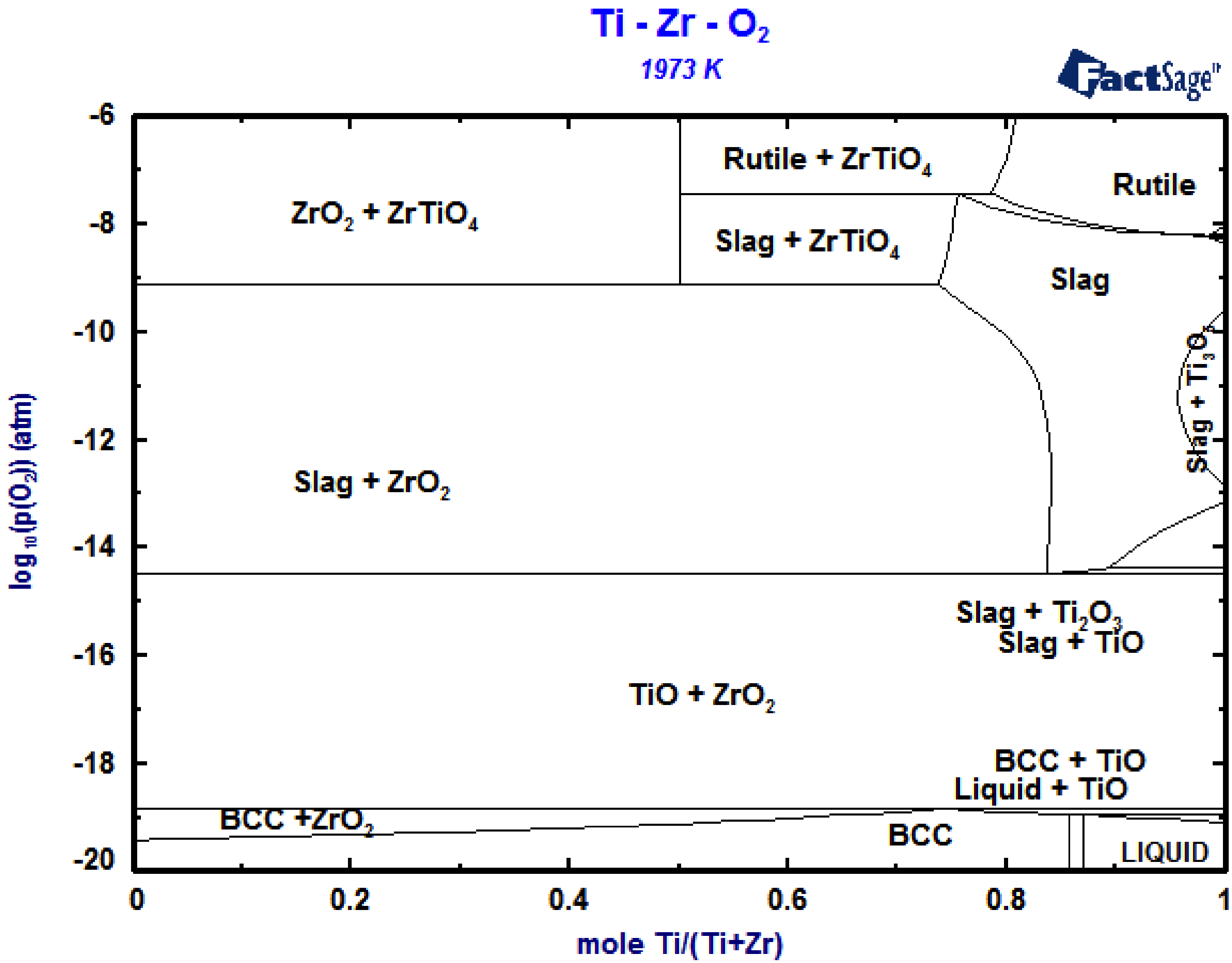

Zr-C-B-Si Quaternary (Proposed by Sorrell-1993)

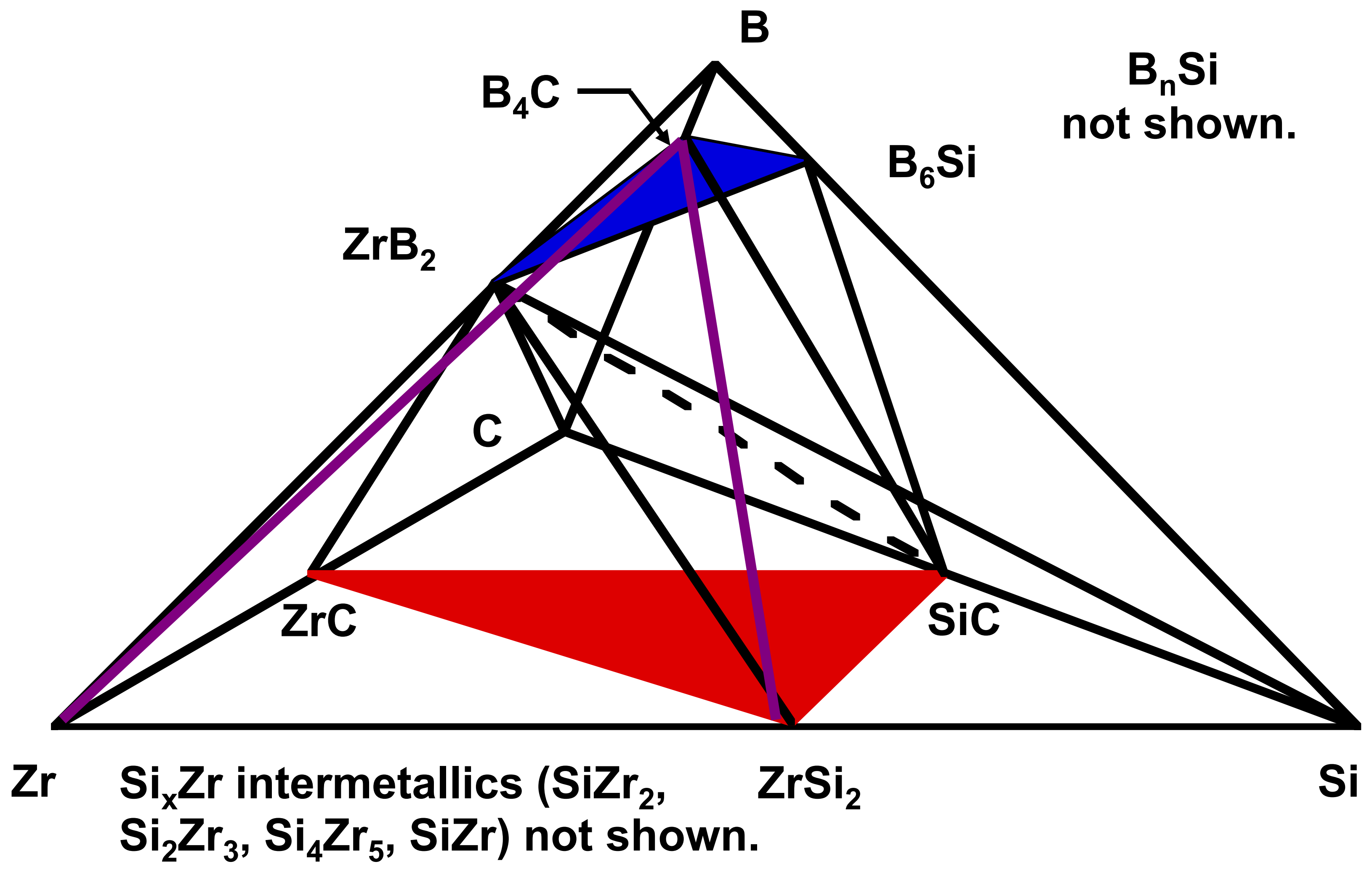

Zr-Si Phase Diagram

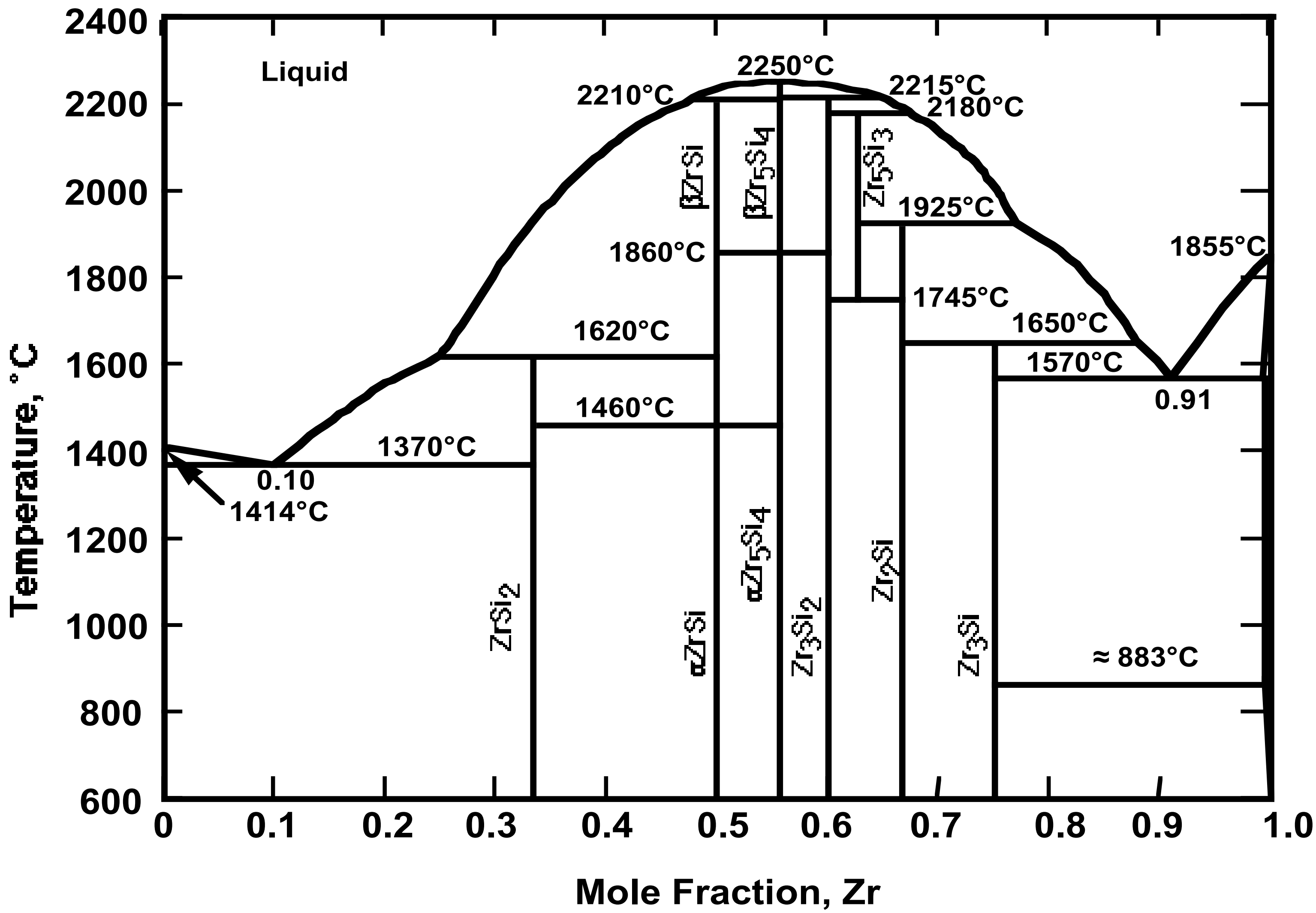

Oxygen Partial Pressure Gradient

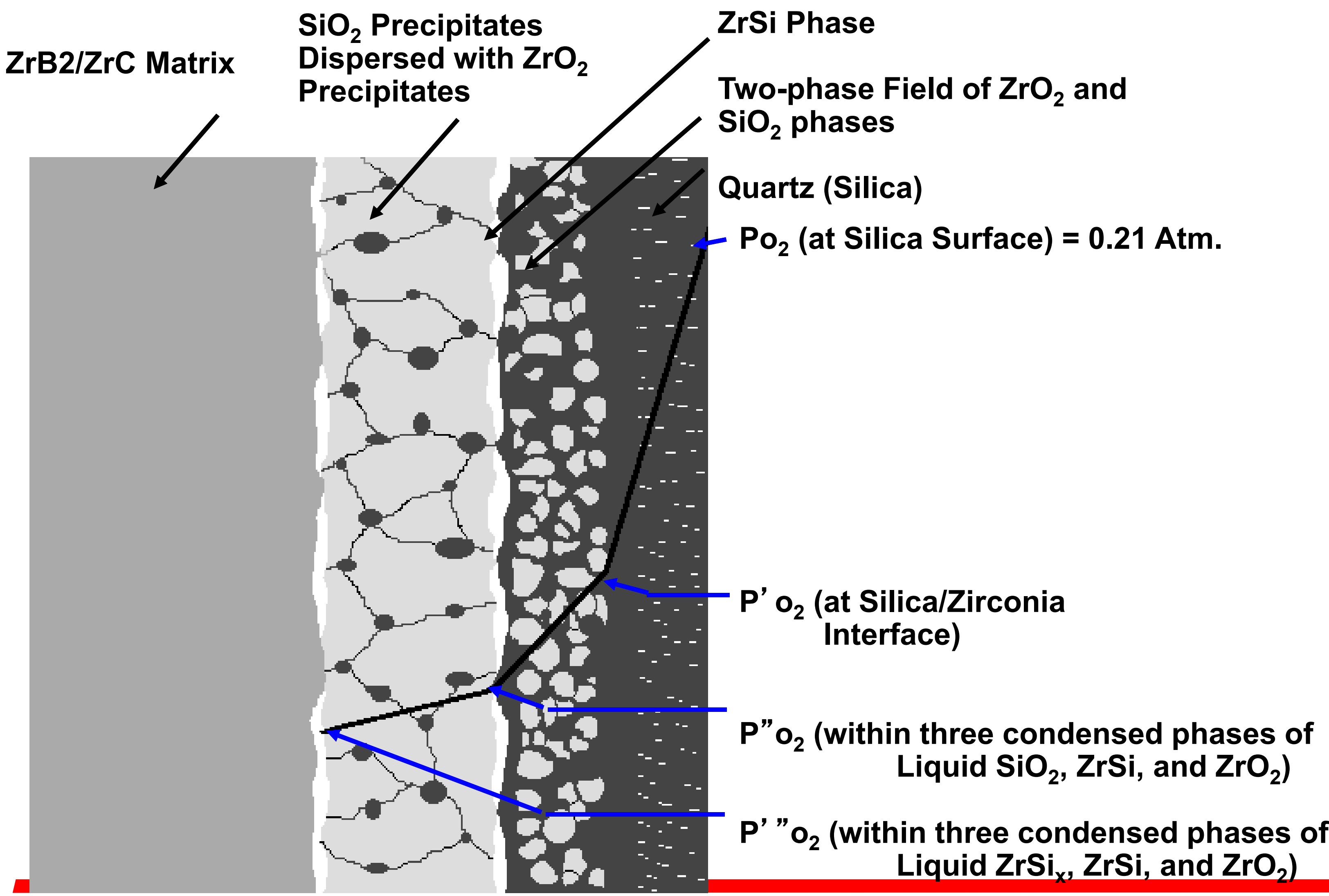

X-FEM Basics

- Extend finite element approximation space to reproduce “difficult” functions.

$$u^{XFEM}(x) = \sum_{I \in \mathcal{N}} N_I(x) u_I + \sum_{J \in \hat{\mathcal{N}}} N_J(x) \Psi(x) a_J$$

Standard Part Enriched Part

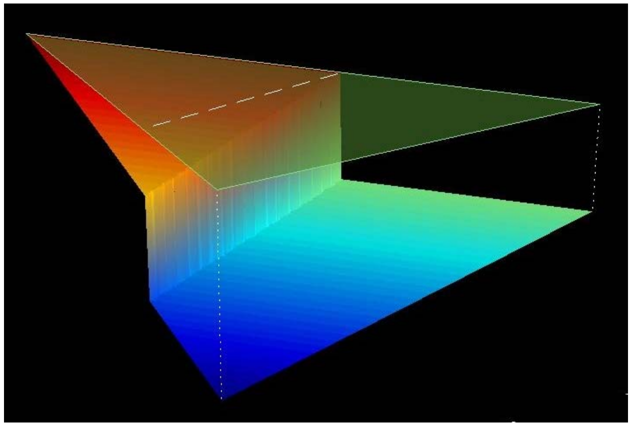

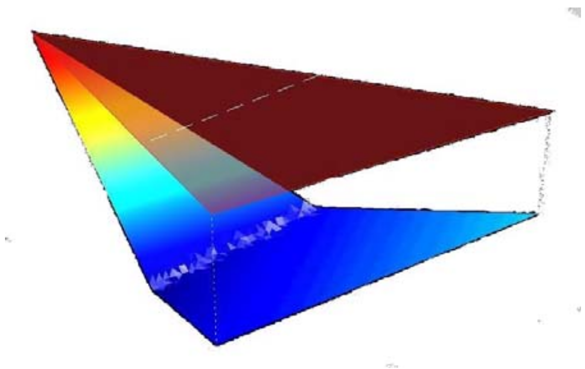

FEA MODEL OF THE MICROSTRUCTURE OF ZrB_2 / ZrC_{1-x} / Zr-Si_x SYSTEM

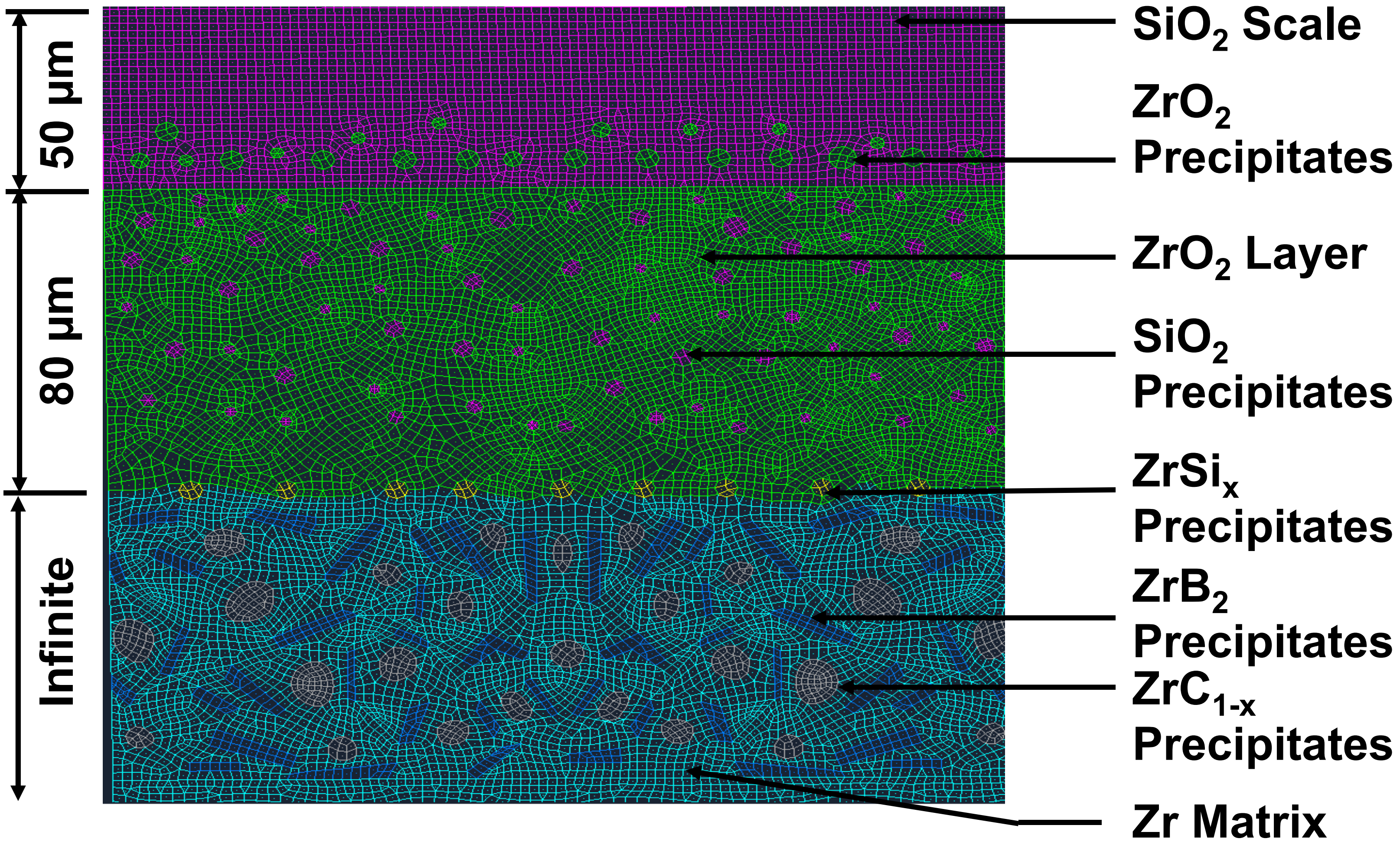

Baseline mesh of the microstructure of ZrB2 / ZrCx / Zr-Si SYSTEM

Optimal Configuration of ZrO_2 Precipitates in SiO_2 Matrix

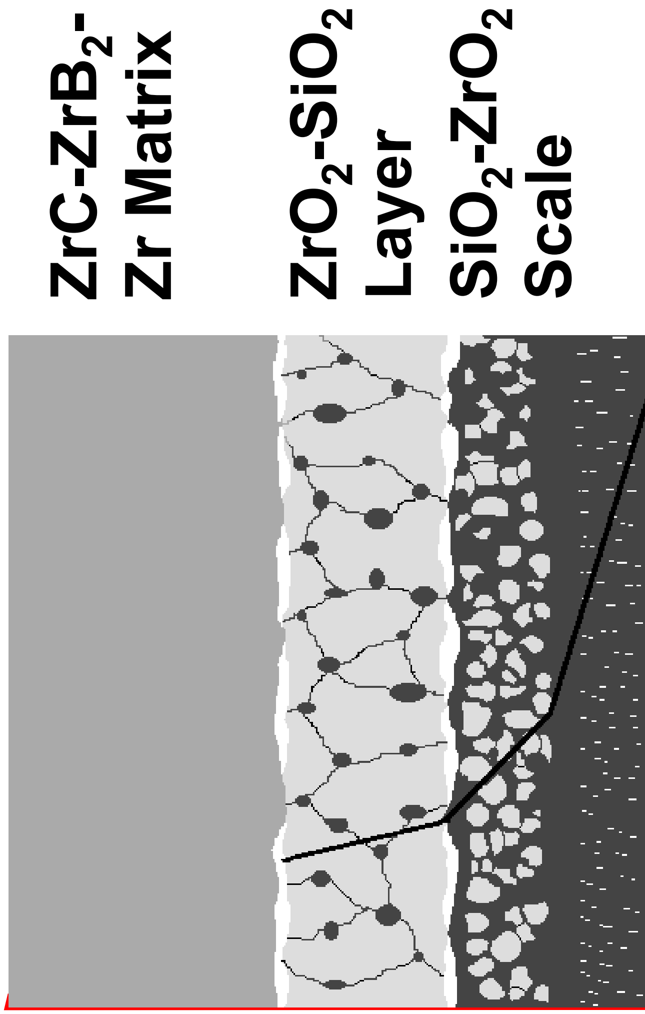

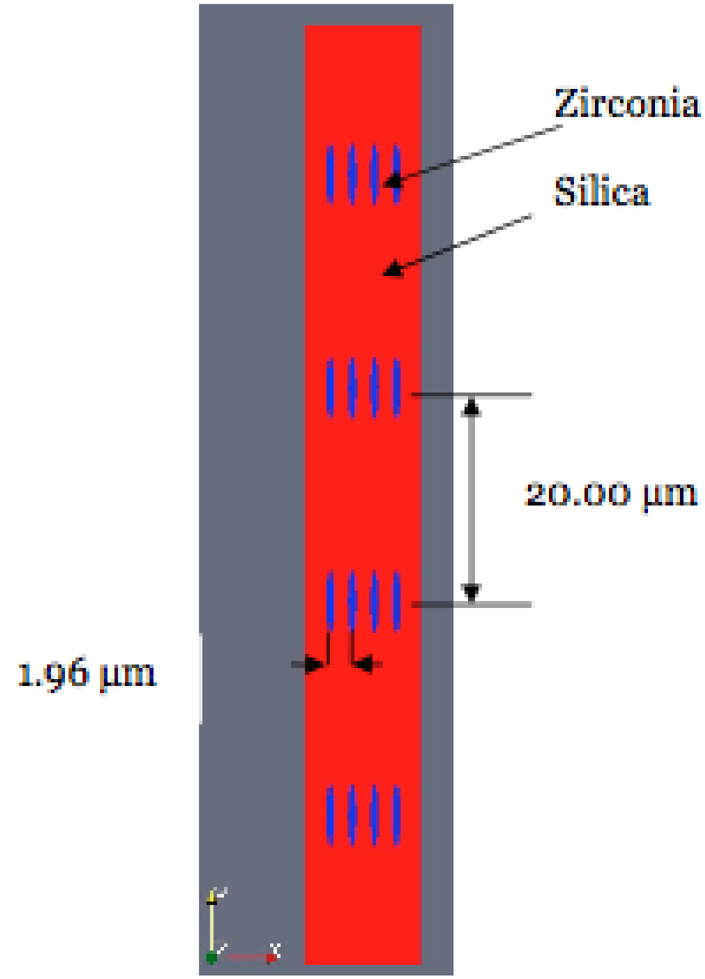

Zr-Si-O Ternary at 1800° C

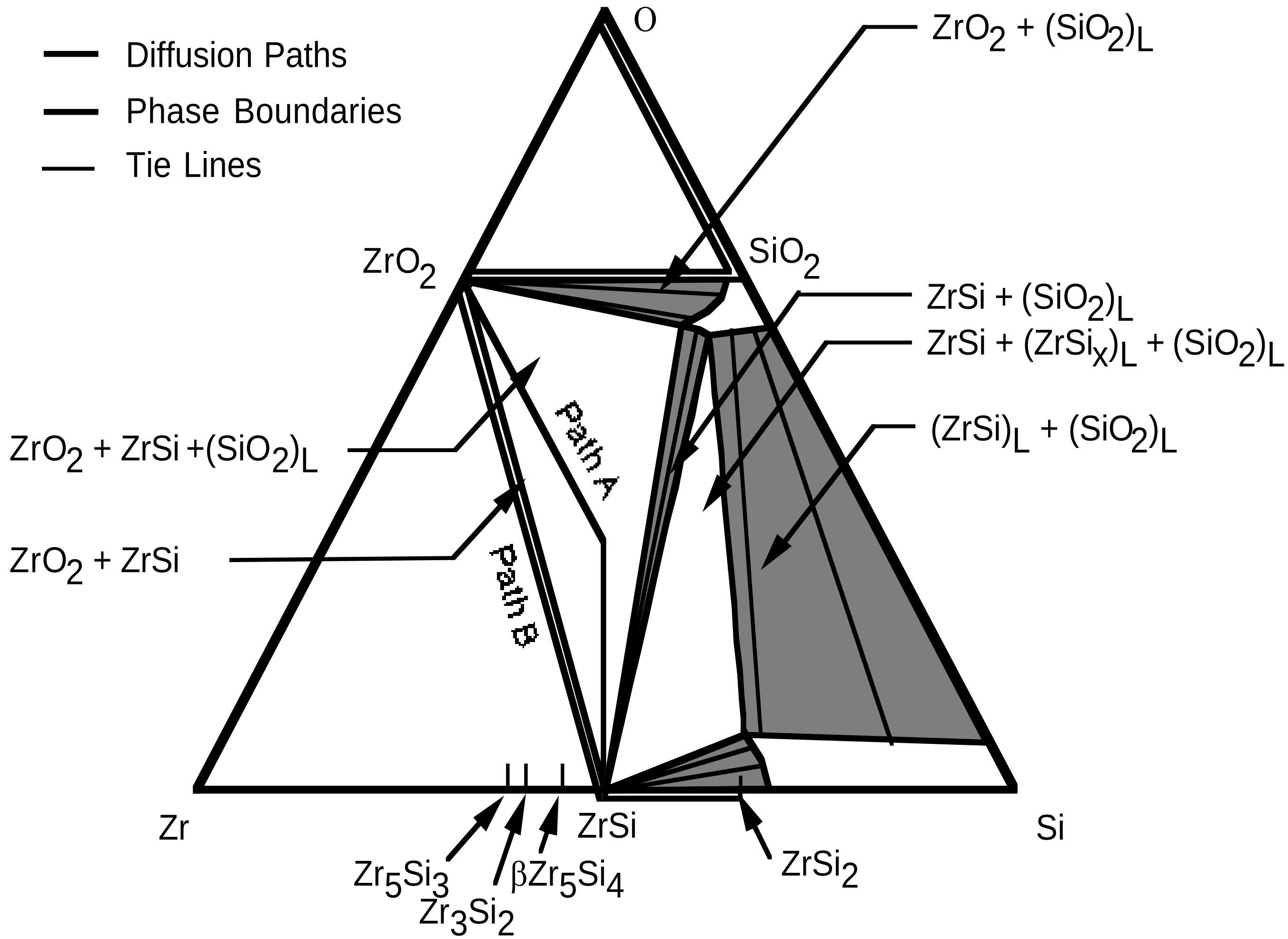

Furnace Assembly

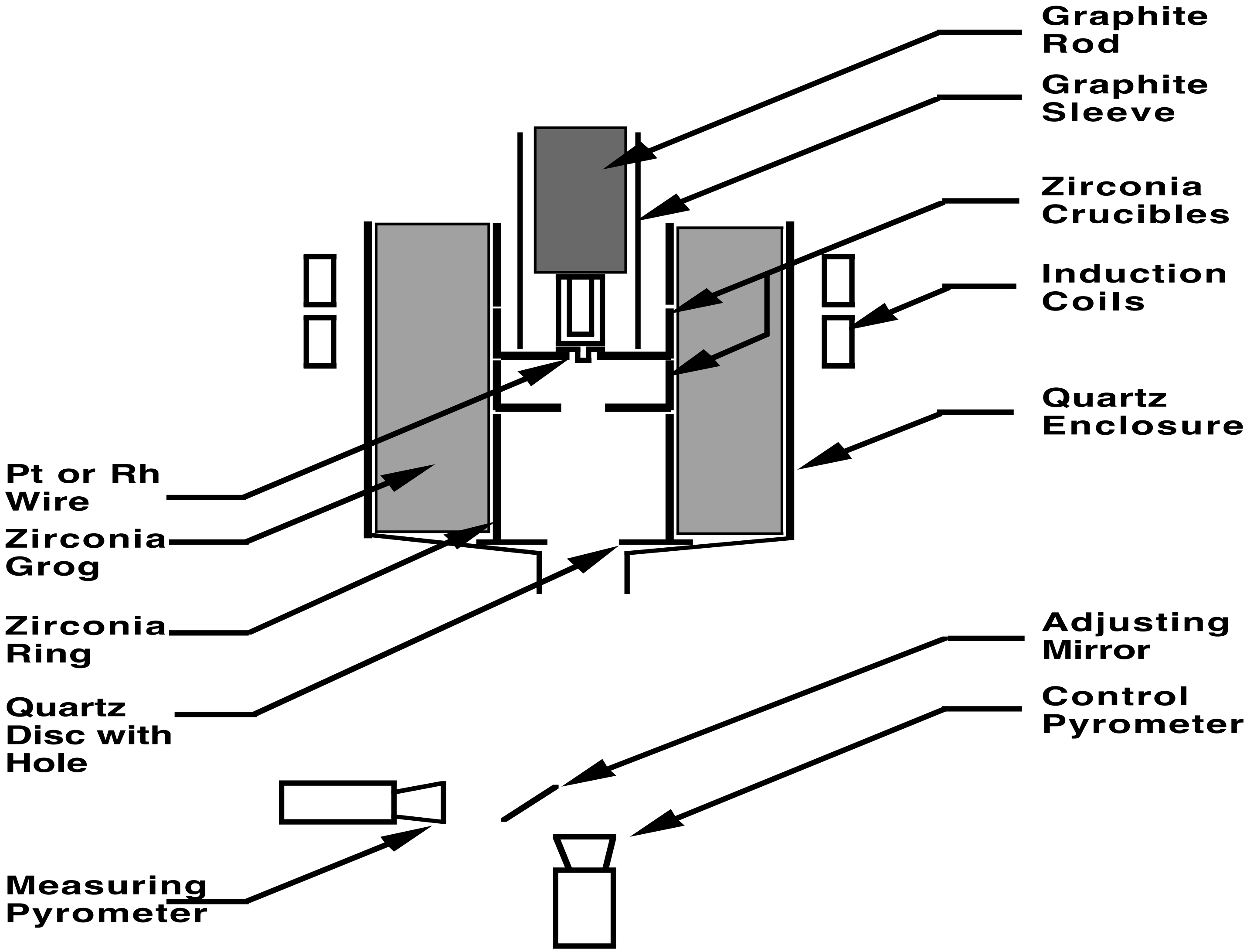

Sketch of Oxygen Diffusion

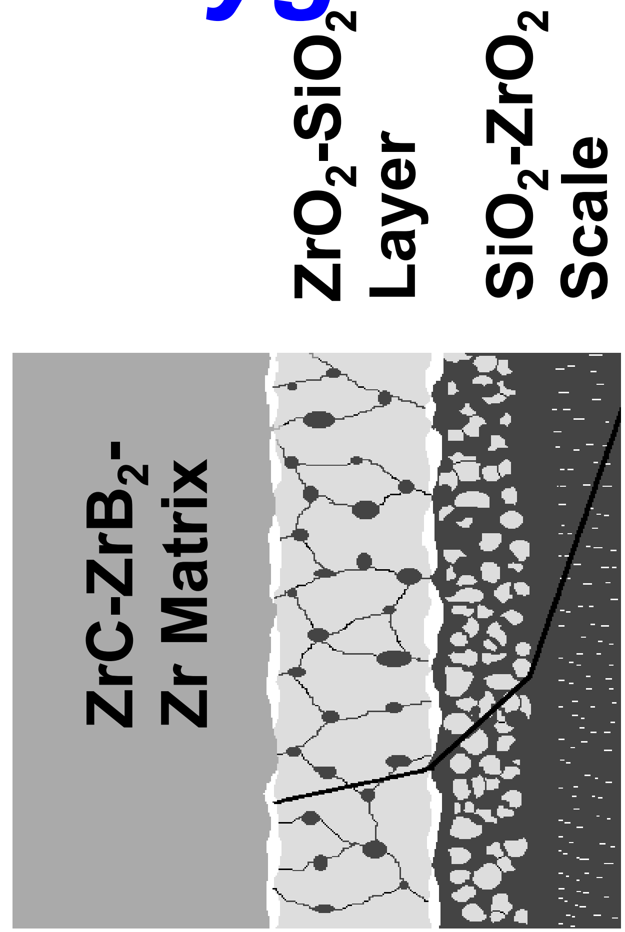

$$D_{Oxygen}^{ZrO_2} > D_{Oxygen}^{SiO_2}$$

Graphite Enclosure in Dielectric Induction Furnace

- Melted previously ZrO_2 (2983 K)
- Control plasma formation with He and flow rate
- Deoxidized Ar and He flows
- Should improve temperature measurement

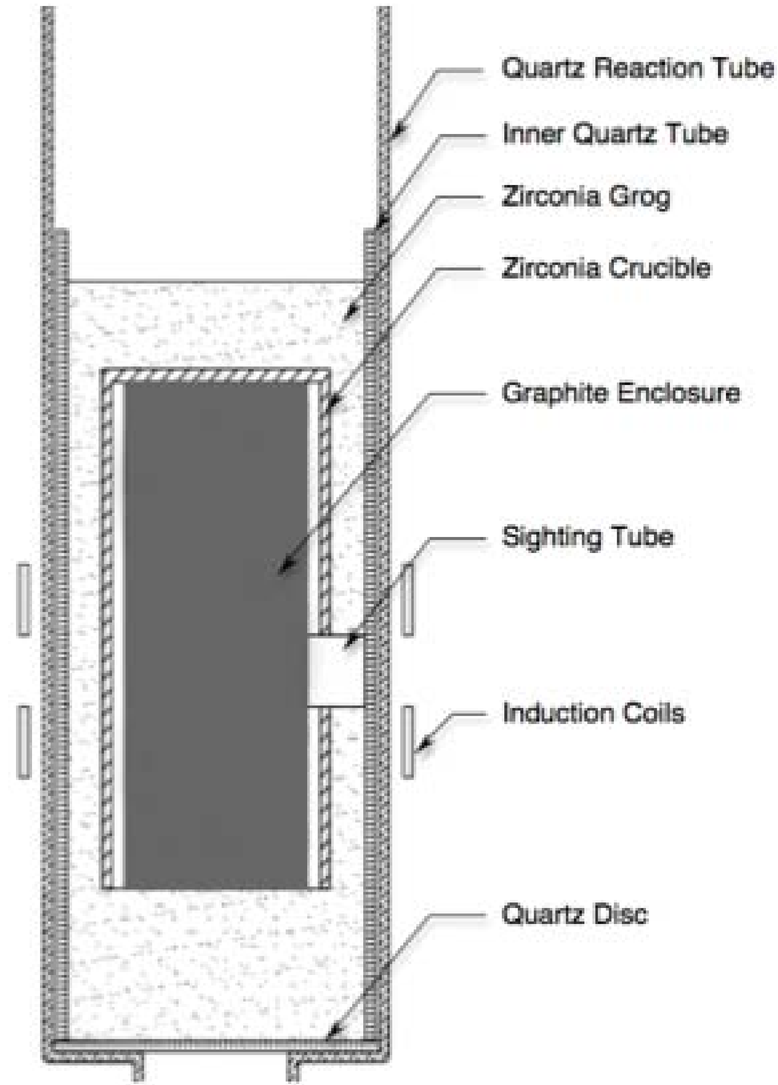

Configuration of Zr alloy/B_4C reaction system

- Zr-Y-Ti alloy reacting with B_4C contained in graphite crucibles at 2000 K plus.
- Closed thermodynamic system controls oxygen potential.
- $Al/Al_4CO_4/Al_2O_3$ establishes p_{O2} at 1000 K (follows concept of Komarek research group using pseudo-isopiestic technique).

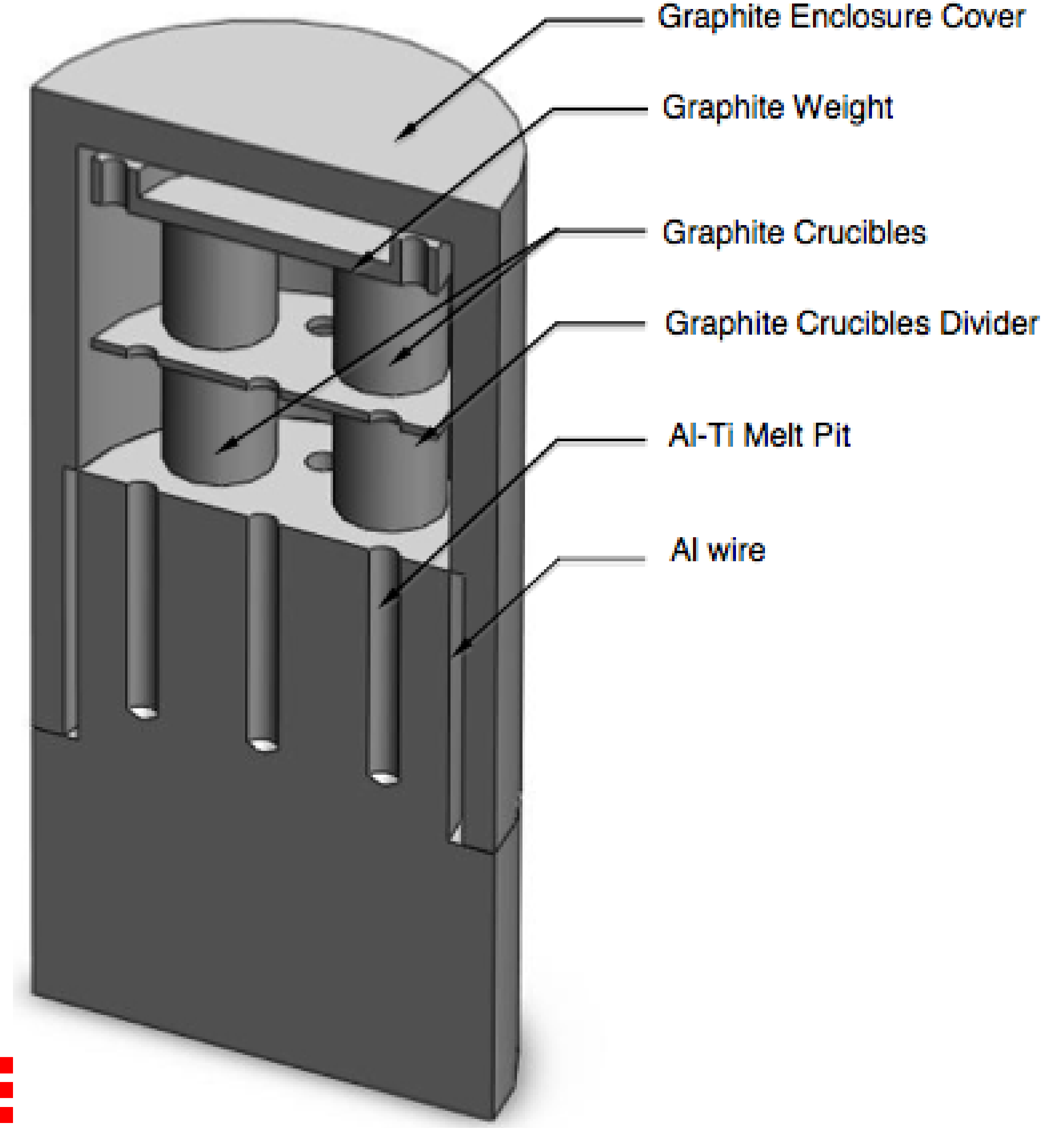

Stability of Al-C-O System at 1000 K and Zr-C-O System at 2500 K

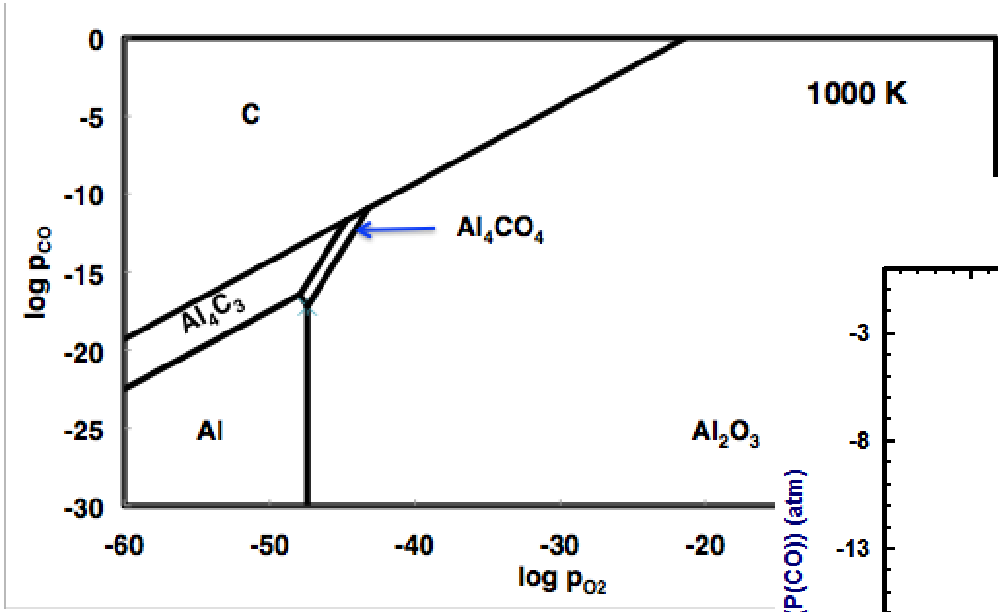

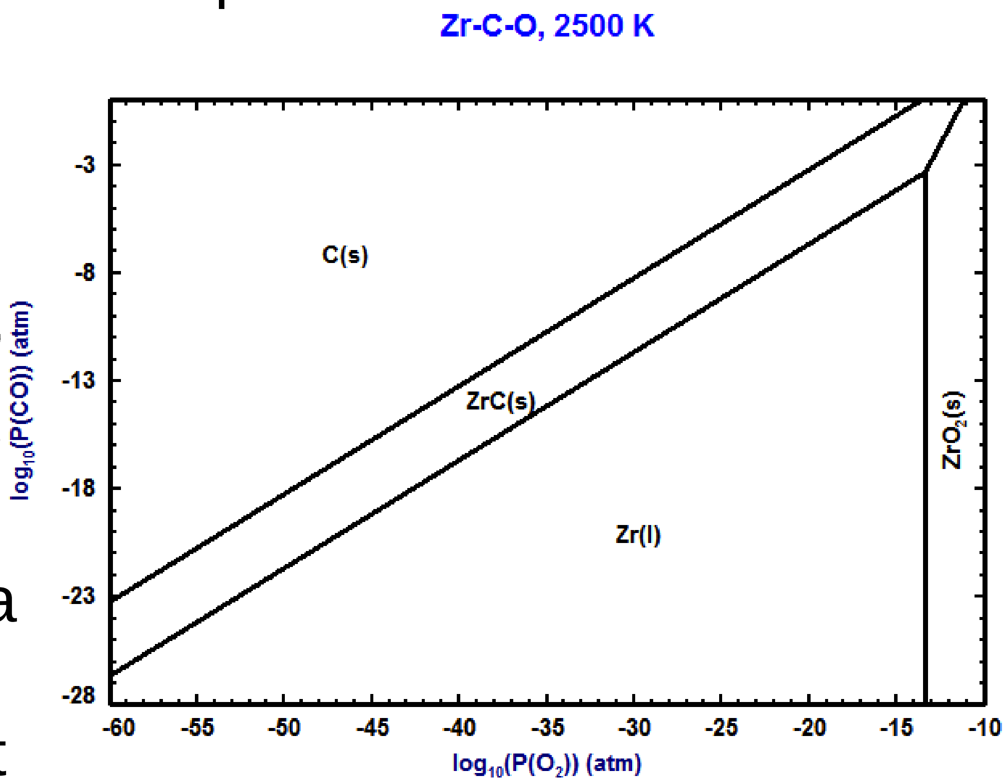

- $Al/Al_4CO_4/Al_2O_3$ estimated at 1000 K for a $p_{O2} = 10^{-47}$ atm
- Zr-Y-Ti alloy/B_4C react at > 2125 K

Diffusional Flux – Kinetics Issues

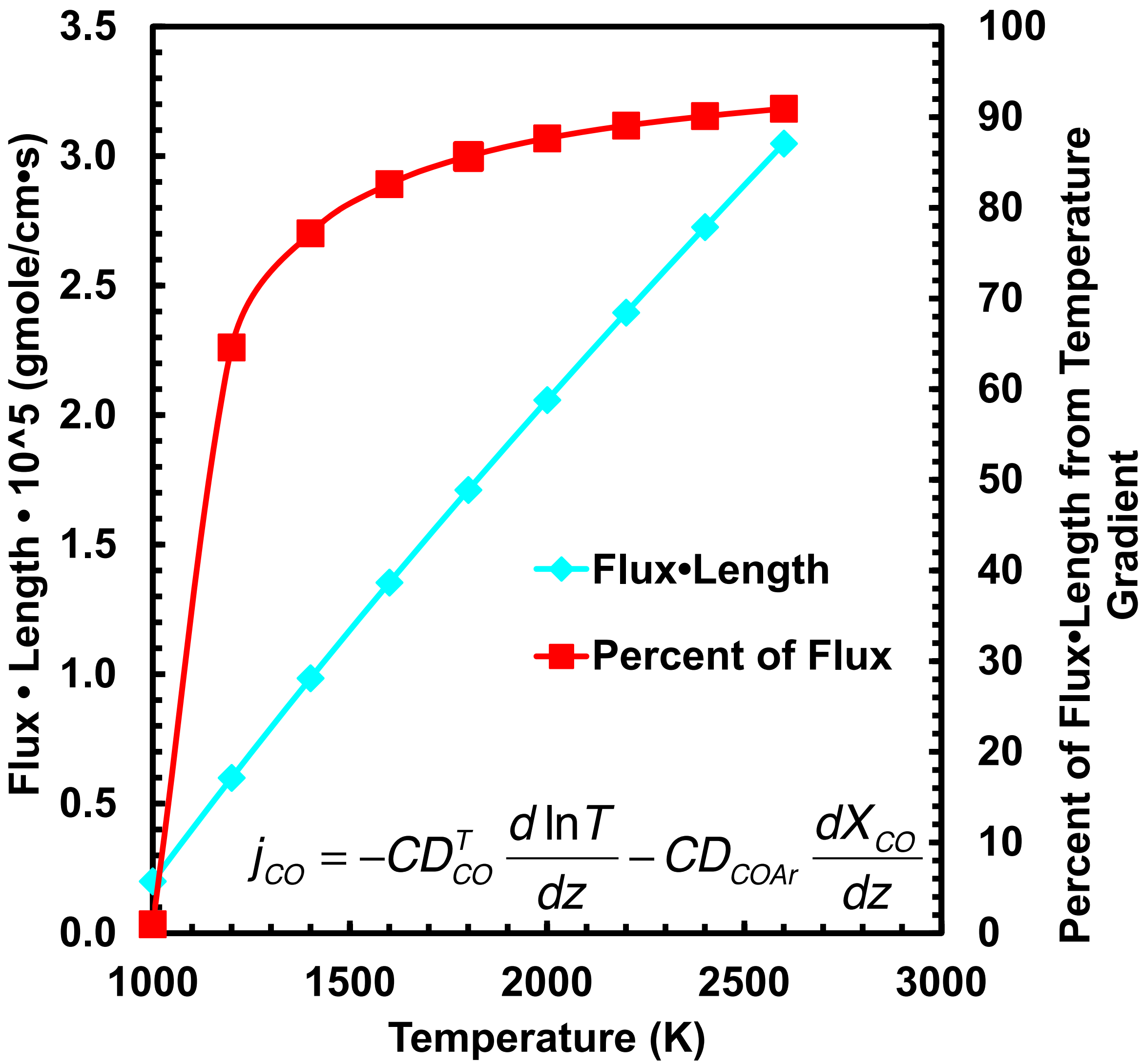

- D_{COAr} from Poirier-Geiger and checked with Chapman-Enskog Eq.
- Mean temperature

$$\frac{T_H T_C}{T_H - T_C}\ln\frac{T_H}{T_C} = 1527K$$

- $Al/Al_2O_3/Al_4CO_4$ reaction rate?

Temperature Measurement of Hf Melt Reacting with B_4C Packed Bed > 2600 °

- Determine effect of dT/dx on infusion (i.e., σ_{LV})
- Determine the effect of ΔT spike on infusion
- Determine dT/dx on metastable phase formations.

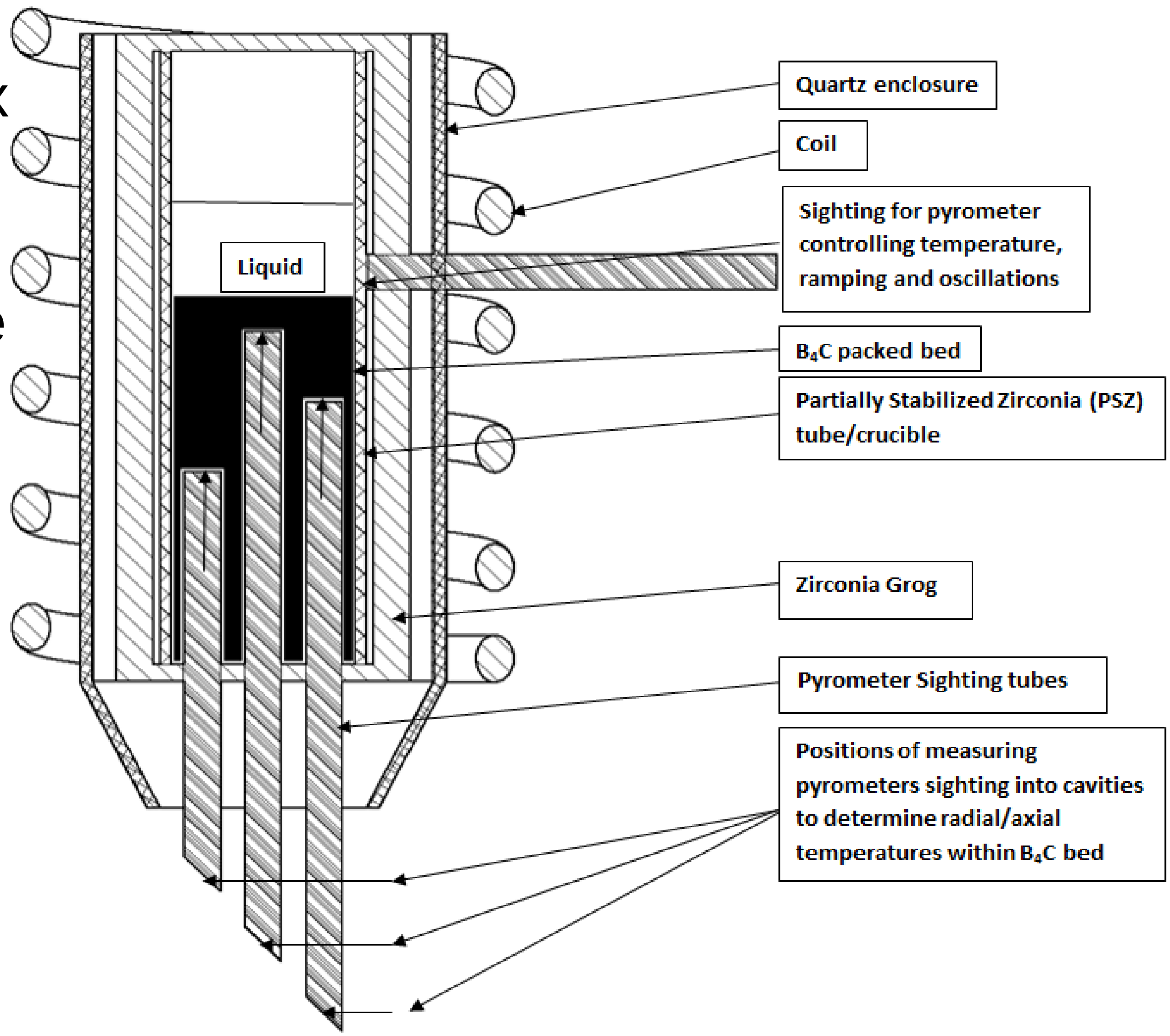

Surface Energies for Hf Alloy Melts Determined from Elements

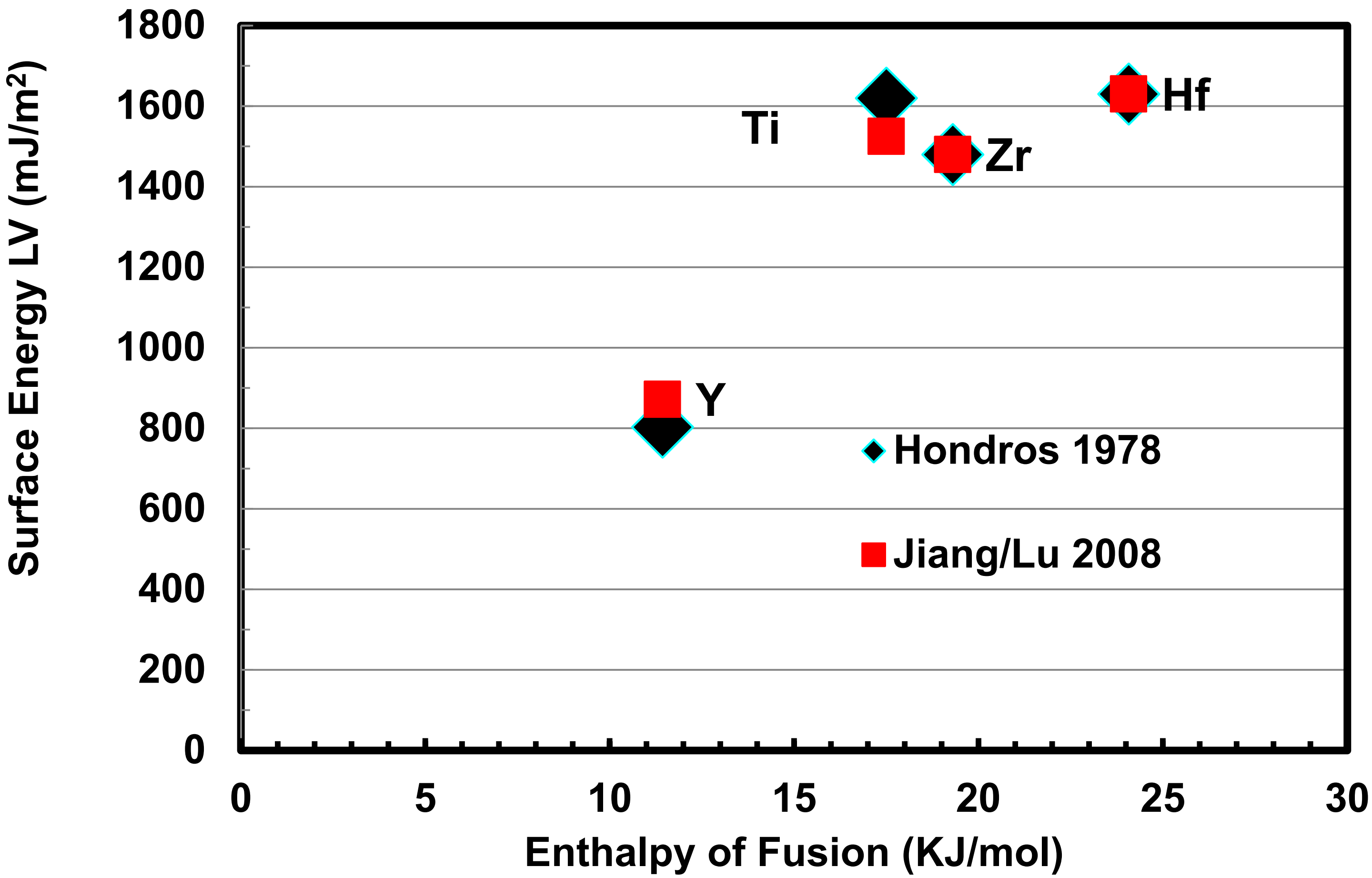

Depth of Infusion into Packed Bed Driven by Surface Energies

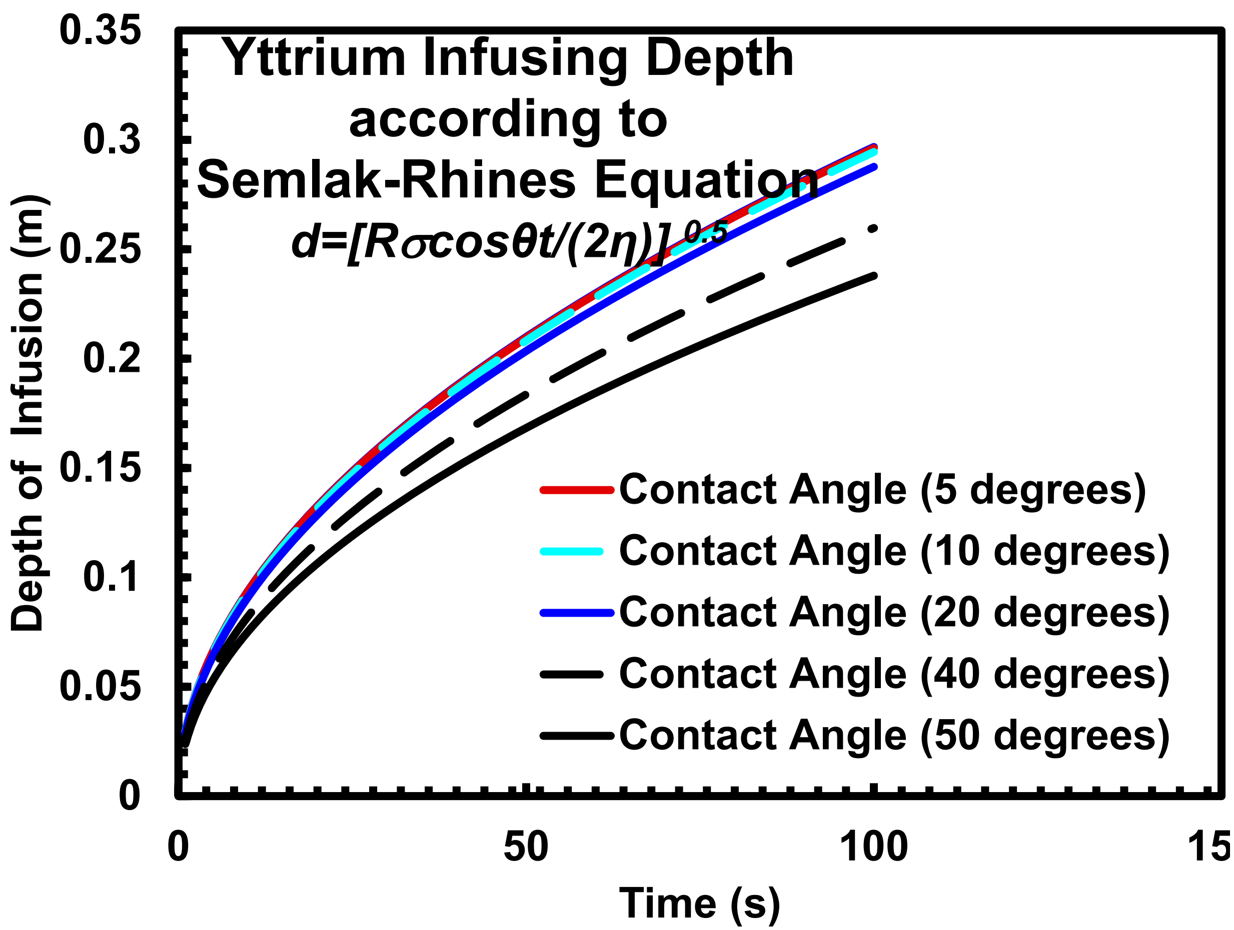

- Expand $d\sigma/dx$ (e.g.,

$$\eta \frac{\partial u_x}{\partial y} = \frac{\partial \sigma}{\partial T} \frac{\partial T}{\partial x}$$

- Use Fluent to model computational fluid dynamics.
- Determine alloying effects (e.g., Hf-Y-Ti)

$$\Gamma_i^{Hf} = -\frac{1}{RT}\left(\frac{\partial \sigma}{\partial \ln p_{O_2}}\right)_{T,i\neq k}$$

- Determine σ with:
  - Butler equation (Yeum, Speiser and Poirier-1989)
  - Multicomponent ΔG incorporating σ using FactSage

Densification of ZrB_2-TiC-Y_2O_3 (with and without Ta) Composites Using Spark-Plasma Sintering at University of Arizona

Dr. Erica L. Corral[1]
Luke S. Walker
Victoria R. Marotto

Dr. Arturo Bronson[2]
Brenda Mota, Carlos E. Castillo
David Pham, Alvaro Sandate

ZrB_2-TiC-Y_2O_3-Ta would react to form ZrO_2-Y_2O_3-TiO_2-Ta_2O_5 determining TiO_2-Ta_2O_5 glassy phase.

[1] Department of Materials Science and Engineering, Arizona Materials Lab, The University of Arizona, Tucson, AZ
[2] Mechanical Engineering Department, The University of Texas at El Paso, El Paso, TX

Joint Work Between the Corral Lab and UTEP in Preparing ZrB_2-based ceramics with additions of Yttria and Ta for Improved Oxidation Resistance Through the Formation of Complex Oxide Scales

Material	Composition (wt%)								
	1	2	3	4	5	6	7	8	9
ZrB_2	79.3	62.0	37.8	33	29	26	30	23	18
TiC	10.3	12.5	15.6	27	36	42	13	19	23
Y_2O_3	10.4	25.5	46.6	40	40	32	37	28	23
Ta*	-	-	-	-	-	-	20	30	36
Temperature (°C)	1600 1650 1700^t 1750	1500 1700 1750	1500 1700 1750	1700	1700	1700	1700	1750	1800

Sample volumes of 1.5 cm^3 from a 20mm die.
* – Ta foil was finely cut and dispersed in the powder
^{t} – 3 samples of this composition produced

Compositions for ZrO_2-Y_2O_3-TiO_2-Ta_2O_5 scales

- In t-ZrO_2/c-ZrO_2 region
- Near c-ZrO_2/t-ZrO_2/$TiO_{2,L}$ region
- Near c-ZrO_2/$Y_2Ti_2O_7$ region
- Ta added for Ta_2O_5-TiO_2 eutectic scale

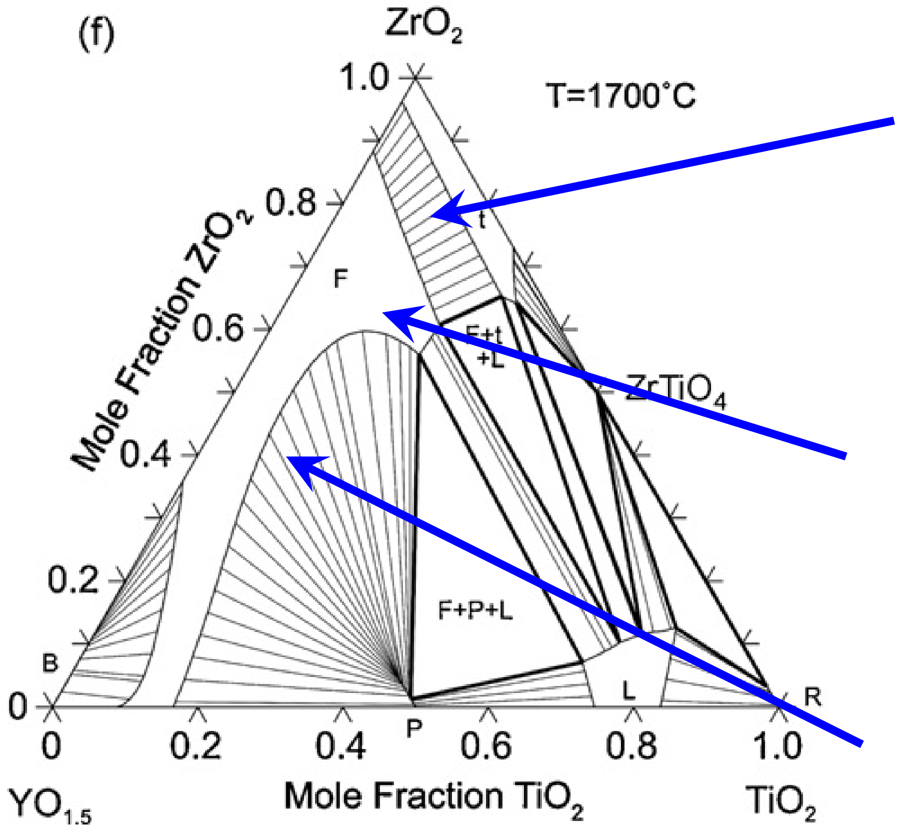

12 TiO_2
10 Y_2O_3
78 ZrO_2

15 TiO_2
23 Y_2O_3
62 ZrO_2

15 TiO_2
45 Y_2O_3
40 ZrO_2

Diagram from Schaedler, Fabrichnaya and Levi -- 2008